VARIABLE-TEMPERATURE ^{1}H-NMR AND AB INITIO STUDY OF 5-AMINO-IMIDAZOLE-4-CARBOXAMIDE (AICA): COMPETING PATHS FOR AMIDE-H SCRAMBLING

A Thesis

presented to

the Faculty of the Graduate School

University of Missouri-Columbia

In Partial Fulfillment

Of the Requirements for the Degree

Master of Science

---

by

YANG LIU

Dr. Rainer Glaser, Thesis Supervisor

DECEMBER 2008

The undersigned, appointed by the dean of the Graduate School, have examined the thesis entitled

VARIABLE-TEMPERATURE ^{1}H-NMR AND AB INITIO STUDY OF 5-AMINO-IMIDAZOLE-4-CARBOXAMIDE (AICA): COMPETING PATHS FOR AMIDE-H SCRAMBLING

presented by Yang Liu,

a candidate for the degree of master of science,

and hereby certify that, in their opinion, it is worthy of acceptance.

Professor Rainer Glaser

Professor Timothy Glass

Professor Ping Yu

ACKNOWLEDGMENTS

Firstly, I would like to show appreciation to my research advisor Professor Rainer Glaser for his guidance, advice, support, constructive suggestions throughout my master study.

Secondly, I would like to express gratitude to my committee members, professors of all divisions for their help, kindness, suggestions and instructions I would like to thank Dr. Wei Wycoff and Dr. Shaokai Jiang for their assistance in NMR analysis. I would also like to acknowledge the department of chemistry for its great graduate training program.

Thirdly, I would like to thank each member of the Glaser research group, for their helps and kindness. I would like to acknowledge John for his guidance and support in my research at the first beginning.

Lastly, I am deeply grateful to my wife for her support throughout my M.S. studies. I would also like to acknowledge my parents and my friends for their assistance and encouragement.

TABLE OF CONTENTS

LIST OF TABLES

LIST OF SCHEMES

LIST OF FIGURES

VARIABLE-TEMPERATURE ^{1}H-NMR AND AB INITIO STUDY OF 5-AMINO-IMIDAZOLE-4-CARBOXAMIDE (AICA): COMPETING PATHS FOR AMIDE-H SCRAMBLING

Yang Liu

Dr. Rainer Glaser, Thesis Supervisor

ABSTRACT

5(4)-aminoimidazole-4(5)-carboxamide (AICA and TAICA) is an important precursor for the synthesis of purines in general and of the nucleobases adenine and guanine in particular. Biotic nucleobase synthesis has been studied in great detail and its chemistry and biochemistry are understood very well. In contrast, hypotheses regarding prebiotic nucleobase syntheses remain controversial. While such studies focused on aqueous solution chemistry for half a century, planetary nucleobase syntheses in frozen solids (ice) and other extreme environments have been explored in the past two decades. Spectacular advances in observational astronomy and the evolving knowledge about the chemistry and physics of the interstellar medium (ISM) suggest new options and the very possibility of prebiotic nucleobase synthesis in the cold ISM.

The discourse about prebiotic chemistry in interstellar space relies on observational astronomy. Hence, precise knowledge is required about the spectroscopic properties of presumed intermediates together with knowledge of their structural preferences and their isomerization dynamics. Here, we report on the structure and dynamics of AICA in a variety of solvents and the gas phase. The interplay between CC- and CN- rotations are discussed as well.

1 Introduction

5-Aminoimidazole-4-carboxamide (AICA) is an important precursor for the synthesis of purines. For example, hypoxanthine can be prepared by cyclization of AICA with a variety of condensation reagents, and adenine then becomes accessible through the pathway shown in Scheme 1.[1] Zubay and Mui[2] recently reported the possible prebiotic synthesis of hypoxanthine via the HCN-tetramer DAMN (Scheme 1) and discussed implications for nucleobase synthesis in the interstellar medium from HCN and water.

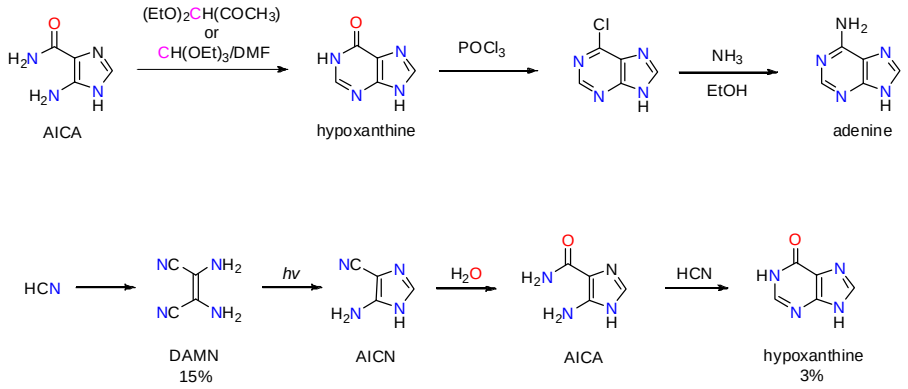

Scheme 1. AICA and nucleobase synthesis.

Observational astronomy showed that many simple organic molecules exist in interstellar space and larger organic molecules are being discovered as the observational sensitivity increases. Meteorites provide a window to the chemistry of protostellar space and the analysis of chondrites,[3] especially of the Orgueil[4] and the Murchison[5,6,7] meteorites, have revealed pyrimidines and purines,[8,4,7] including the nucleobases. Compelling arguments have been made regarding the survivability of organic compounds during extraterrestrial delivery via carbonaceous chondrites.[9] Moreover, recent measurements of carbon isotope ratios have established the non-terrestrial origin of uracil and xanthine in the Murchison meteorite.[10]

Chemical analyses of organic matter in meteorites have not provided any indication of AICA and this would be expected.

The detection of AICA in interstellar space would greatly advance the hypothesis of prebiotic hypoxanthine in interstellar space. Vibrational spectroscopy provides the most likely method for the detection of large organic molecules and the prediction of the vibrational signature of AICA requires knowledge of the molecular conformation.

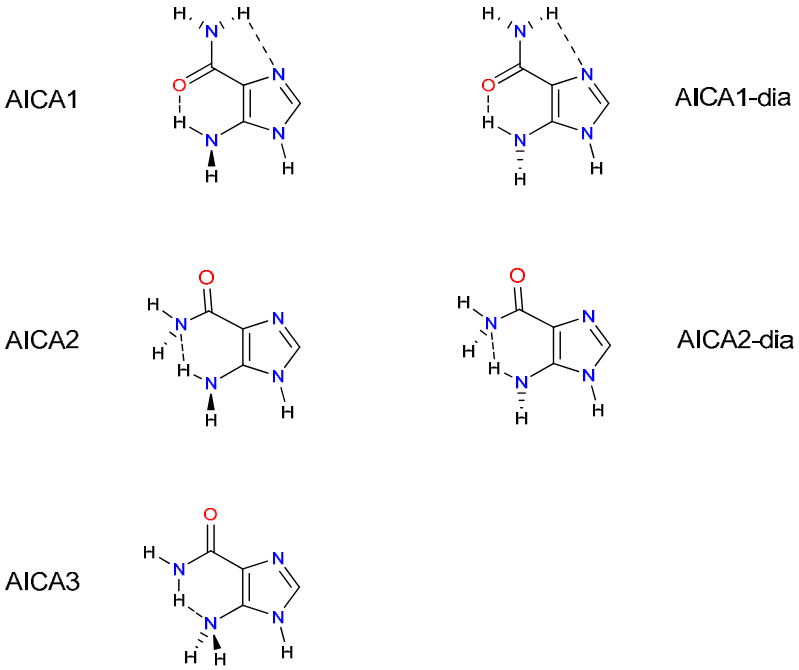

Scheme 2. Nomenclature for stereoisomers of **AICA** and intramolecular hydrogen bonding (HB).

Here, we report the results of a variable-temperature ^{1}H-NMR measurements in acetone and acetonitrile to determine the conformation of AICA and to study its stereochemical dynamics. The experimental data are interpreted in light of the results of extensive ab initio studies of AICA and potential energy surface analyses were performed both for the free molecule in the gas-phase and with consideration of solvation. The potential energy surface analysis included the consideration of the five minima shown in Scheme 2 and all the relevant paths for their interconversions. We will show that the amino-N inversions of AICA1 to AICA1-dia and AICA2 to AICA2-dia are very fast. Hence, three distinct stereoisomers exist and we will show

that AICA1 is the most stable one. The stereoisomer AICA1 occurs in solutions of acetone and acetonitrile and this finding is in line with results of crystallographic studies. Stereoisomers AICA2 and AICA3 both play roles in the dynamics of AICA1.

2 Experimental and Computational Methods

2.1 NMR Measurements

Chemicals and Solvent:. AICA hydrochloride (98%) was purchased from Acros Organics. $(CD_3)_2CO$, CD_3CN and $CDCl_3$ were obtained from Cambridge Isotope Laboratories, Inc.

Instrumentation. Variable temperature (VT) NMR experiments were carried out on a Bruker Avance DRX300 NMR spectrometer equipped with a 5 mm broadband probe and a BVT-3000 VT controller. The sample tube was placed into the probe using a ceramic spinner. Dry air (for measurements above RT) or liquid nitrogen was used as VT control gas. The sample was allowed to equilibrate at each desired temperature for 5 - 10 minutes before the start of shimming and acquisition. Generally, VT NMR measurements were performed by raising the temperature until coalescence is observed and then again by lowering the temperature in 10-degree steps until just above the freezing point of the solution. The temperature ranges were 45 to -70 ºC for acetone-d6 and 50 to -45 ºC for acetonitrile-d3. For each sample, either 16 or 32 scans were acquired to reach sufficient signal intensity. A 2-Hz line broadening was applied to each FID before Fourier transformation. The residual proton signals of acetone (2.04 ppm rel. to TMS) and acetonitrile (1.93 ppm rel. to TMS) were used as chemical shift standard.

Sample Preparation. The following is the purification method employed in our lab to get free AICA base. Methanol (30 mL) was added into a flask. Then 500 mg AICA·HCl and the molar equivalent potassium carbonate were dissolved in the methanol and stirred for half an hour. The solution was evaporated to a volume of

ca.1 mL. The concentrated product was purified by column chromatography on silica gel using CH_3OH/CH_2Cl_2 (80 : 20 v/v) as an eluent. After evaporation of solvent, the product was dried on a Schlenk line.

Determination of the Activation Barrier. [11] For uncoupled signals, the Gutowsky-Holm equation, $k_c = \pi\ \Delta\nu(T_c)$ / SQRT(2), relates the exchange rate of nuclei A and B to the NMR line separation $\Delta\nu$ at the coalescence temperature T_c. The value $\Delta\nu(T)$ provides the difference between the Larmor frequencies of the two sites A and B in a given exchange system, and the coalescence temperature T_c is the lowest temperature at which the two signals of the AB system merge to appear as one single peak. In the slow-exchange temperature range, the measurements of $\Delta\nu(T)$ are linear in T, $\Delta\nu = aT + b$, and linear regression and extrapolation afford T_c and $\Delta\nu(T_c)$. With the data of Table 1, we determined $\Delta\nu$ at T_c with high precision and derived k_c. Substituting k_c and T_c into the Eyring equation, $k = \kappa(k_bT/h)\exp(-\Delta G^{\neq}/RT)$, assuming the transmission coefficient κ to be unity, one obtains $\Delta G^{\neq}(T_c) = 4.575\cdot10^{-3}\ T_c\ [10.319 + \log\ (T_c/k_c)]$ in units of kcal/mol. This equation can be used to compute the free energy of activation at T_c of an equally populated uncoupled two-site exchanging system and the activation barriers determined in this way are listed in Table 2.

2.2 Potential Energy Surface Analysis.

Ab initio calculations were carried out on a 64-processor SGI Altix 3700 Bx2 system with the program Gaussian03.[12] The potential energy surface analysis was performed with the concomitant inclusion of correlation and solvation effects.

Stationary structures were optimized using second-order Møller-Plesset perturbation theory[13] (MP2) in conjunction with the fully polarized, diffuse function augmented, triply-split 6-311++G** basis set. [14] Vibrational analyses were performed at same level of theory to obtain thermodynamic data and to ensure that the located minima and transition state structures indeed are stationary and have the desired number of imaginary vibrational modes. In addition, the MP2/6-311++G** potential energy surface was explored extensively to determine isomerization paths.

The potential energy surface was scanned to determine the profiles for rotations of both amino groups and of the carboxamide group. The potential energy surface scans were performed in mass-weighted modified redundant coordinates with complete structural optimization at every point.[15]

The energetic effects of solvation frequently are computed at the solvent model level (SML) for the structure optimized with the gas-phase model level (GML), that is, in so-called single point calculations at the SML//GML level. Particularly in the case of molecules with soft modes, solvation can affect structures and we have performed structure optimizations and vibrational analyses at the solvent model level. We employ a self-consistent reaction field (SCRF) solvation model, that is, a polarizable continuum model (PCM) is employed to compute the impact of the implicit solvent environment on the characteristics of molecule within its solvent cavity. More specifically, we employ the PCM method by Tomasi et al.[16] and the cavity is generated by a series of interlocking spheres using the "United Atom Model" (UAO).[17] The solvents of interest here are acetone and acetonitrile and their dielectric constants[18] are $\varepsilon(CH_3COCH_3) = 20.7$ and $\varepsilon(CH_3CN) = 36.64$, respectively. The computation of the solvation energy requires the electron density of the solute and we employed the MP2(full)/6-311++G** level description of the solute, i.e., PCM(MP2(full)/6-311++G**).

Total energies E and the thermodynamic parameters vibrational zero-point energy $VZPE = TE(0\ K)$, thermal energy $TE = TE(298.15\ K)$, and molecular entropy $S(298.15\ K)$ are reported in appendix (Tables A1 and A2) for all minima and transition state structures. Relative energies computed for the gas phase and for acetone and acetonitrile solution, respectively, are listed in Tables 6 and 7, respectively. They include ΔE, $\Delta E_0 = \Delta E + \Delta VZPE$, $\Delta H_{298} = \Delta E + \Delta TE$, and $\Delta G_{298} = \Delta H_{298} - 0.298 \cdot \Delta S$. Complete sets of Cartesian coordinates of all optimized structures in the gas and solution are provided in the appendix of this thesis.

3 Results and Discussion

3.1 Variable-Temperature ^{1}H-NMR Spectra

VT ^{1}H-NMR spectra of AICA in acetone and acetonitrile are shown in Figure 1, and NMR chemical shift data are reported in Table 1. One single stereoisomer is observed and the spectra are assigned to stereoisomer AICA1 (Scheme 4).

Figure 1. Temperature-dependent H-NMR Spectra of **AICA** in (a) D_6-Acetone and (b) D_3-Acetonitrile.

(a)

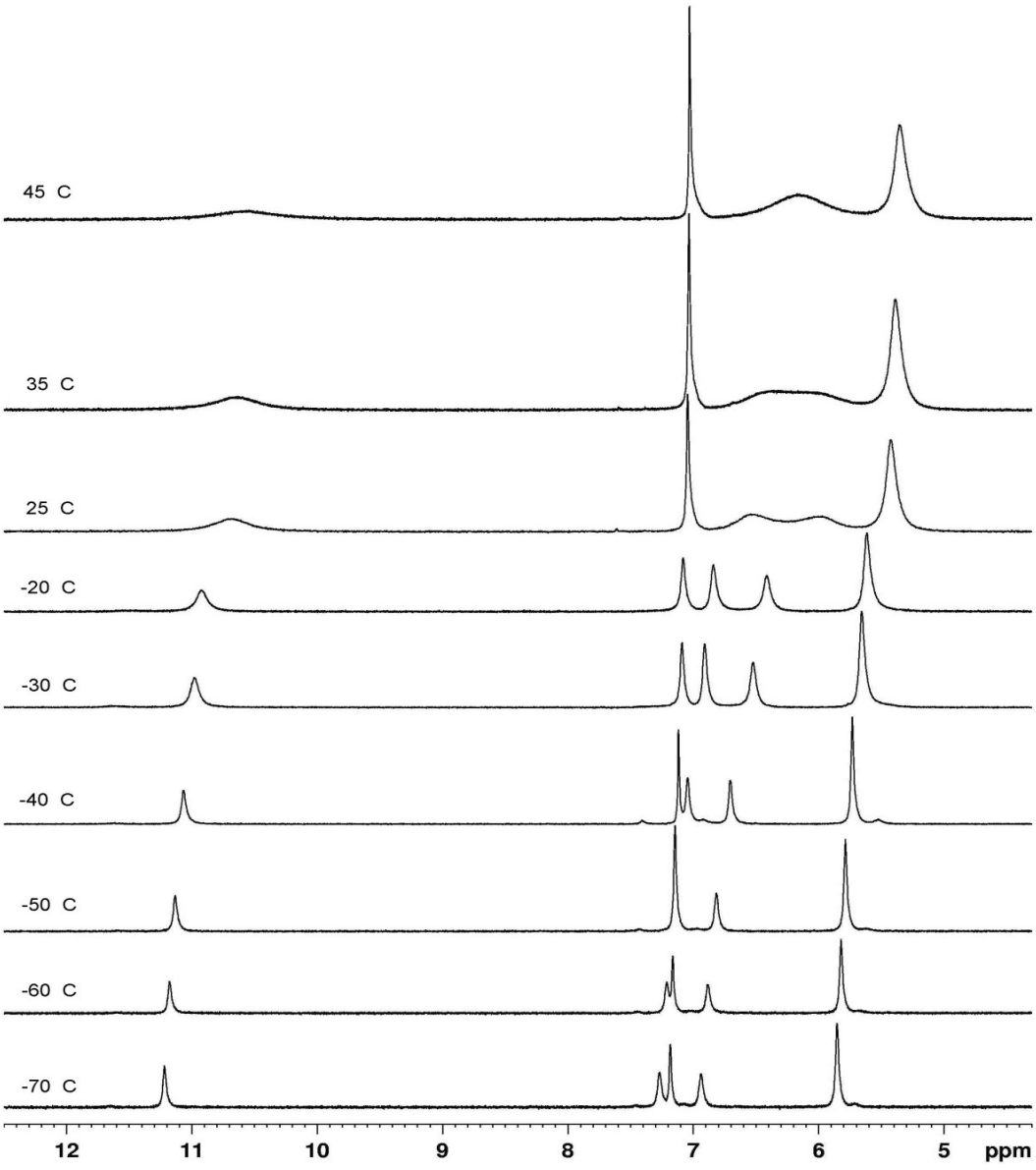

Figure 1. (Continued, place to the right of (a))

(b)

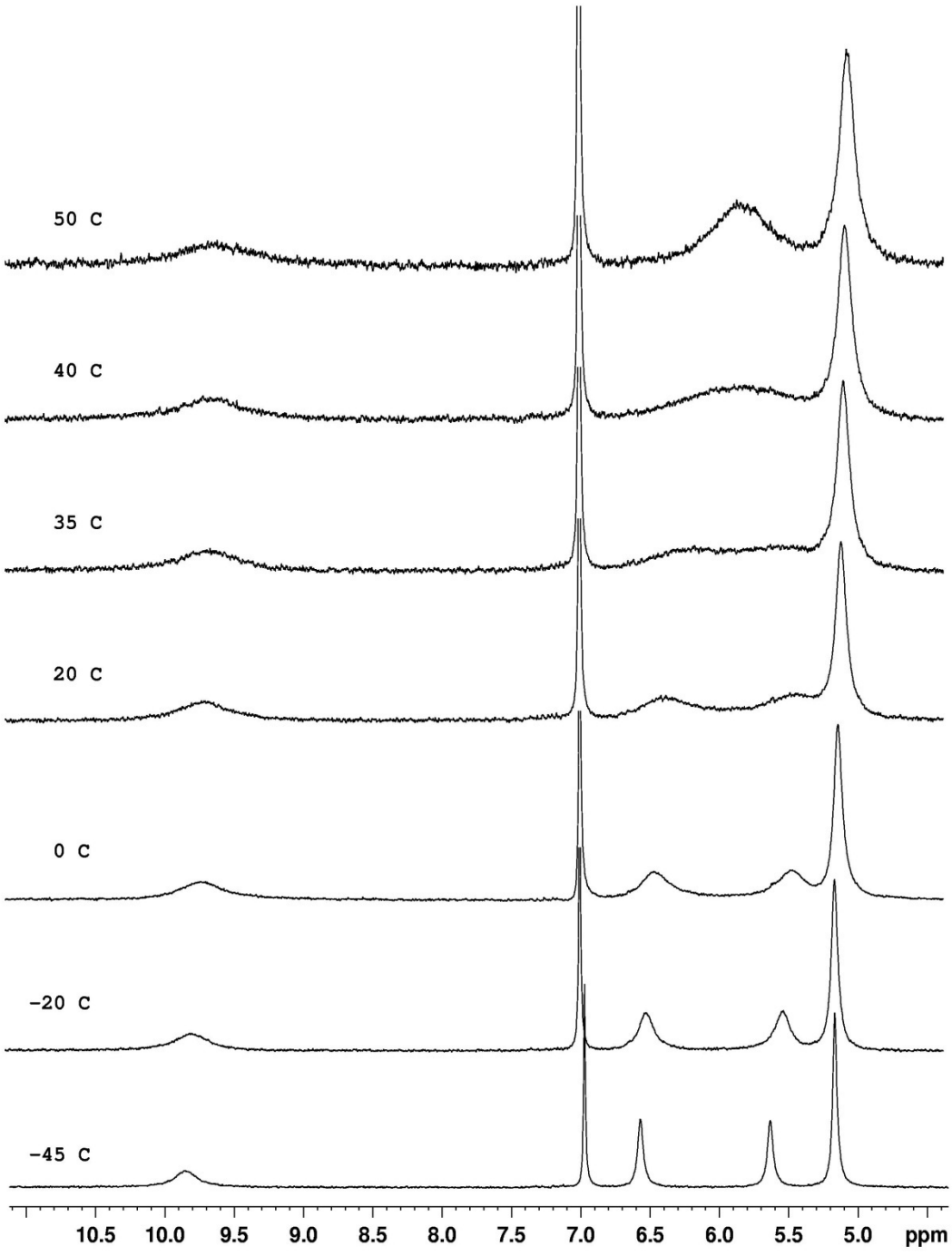

Table 1. Temperature-Dependent H-NMR Data.[a,b]

T (K)	a,δ(NH)	b,δ(CH)	c,δ(NH_2)	d,δ($CONH_2$)	e,δ($CONH_2$)	$\Delta\nu$ (Hz)	κ (s^{-1})
Acetone							
318 (T_c)	10.58	7.03	5.35	6.17		190.9	420.0
308	10.63	7.04	5.39	6.38	6.16	64.5	143.3
298	10.69	7.05	5.43	6.55	5.97	172.5	383.2
253	10.93	7.08	5.61	6.84	6.42	127.2	282.6
243	10.98	7.09	5.66	6.91	6.52	115.8	257.3
233	11.07	7.12	5.73	7.05	6.71	102.3	227.3
223	11.13	7.15	5.79	7.15	6.82	98.4	218.6
213	11.18	7.17	5.82	7.21	6.89	98.7	219.3
203	11.22	7.18	5.85	7.27	6.94	98.7	219.3
Acetonitrile							
323	9.59	6.98	5.05	5.84			
313 (T_c)	9.69	6.98	5.06	5.86		335.7	745.8
308	9.64	6.98	5.07	6.15	5.60	164.4	365.2
303	9.64	6.98	5.08	6.32	5.47	255.3	567.2
293	9.70	6.98	5.09	6.35	5.40	284.7	632.5
283	9.66	6.98	5.10	6.41	5.41	300.0	666.5
273	9.71	6.98	5.11	6.44	5.44	299.7	665.8
253	9.79	6.97	5.14	6.50	5.51	297.0	659.8
243	9.77	6.97	5.15	6.52	5.55	291.0	646.5
233	9.83	6.97	5.16	6.55	5.60	284.7	632.5
228	9.86	6.97	5.17	6.57	5.63	280.8	623.9

Table 2. Measured and Computed Barriers[a]

	Gas-Phase $\varepsilon = 1$	Acetone $\varepsilon = 20.7$	Acetonitrile $\varepsilon = 36.6$
VT-NMR, amide		14.83	14.24
A1-Rotation	16.61	15.63	14.74
A2-Rotation	7.40	10.15	10.39
A1/**A2** Isomerization	11.55	8.68	7.72
A1/**A2** Isom. & **A2**-Rot.	17.26	15.43	14.51

[a] Barriers (ΔG_{act}) in kcal/mol.

Numbering system based on IUPAC for AICA structure is shown in Scheme 3, in order to help assign each characteristic NMR absorbing peak.

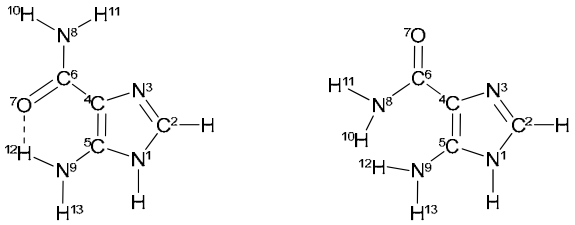

Scheme 3. Selected atom numbering of AICA.

The chemical shift of the sharp peak ca. 7 ppm is essentially independent of the solvent and it is therefore easily assigned to the H atom at C(2). The signal at ca. 10 ppm corresponds to the H atom at N(1), its chemical shift is solvent-dependent, and the peak shows the expected flattening as the rate of exchange with temperature increases. The signals of the amino groups show the most interesting dependencies both on temperature and solvent. The rotation of the amide-amino group is markedly hindered and at low temperatures the amide-H scrambling is slow enough to allow for the observation of well-separated peaks in the region 6 - 7.5 ppm. These peaks broaden with increasing temperature until coalescence is reached at T_c. = 318 K in acetone and at T_c. = 313 K in acetonitrile, respectively. The measured rotational barriers for AICA in acetone and acetonitrile are 14.83 and 14.24 kcal/mol, respectively (Table 2). The rotation of the amino group at C(5) is essentially free and the amino-H atoms cause one signal at ca. 5 - 6 ppm. This amino-H signal is sharp at low temperatures and it is very important to note that this peak broadens quite significantly as the temperature increases and that this peak also shows a solvent-dependent shift with increasing temperature.

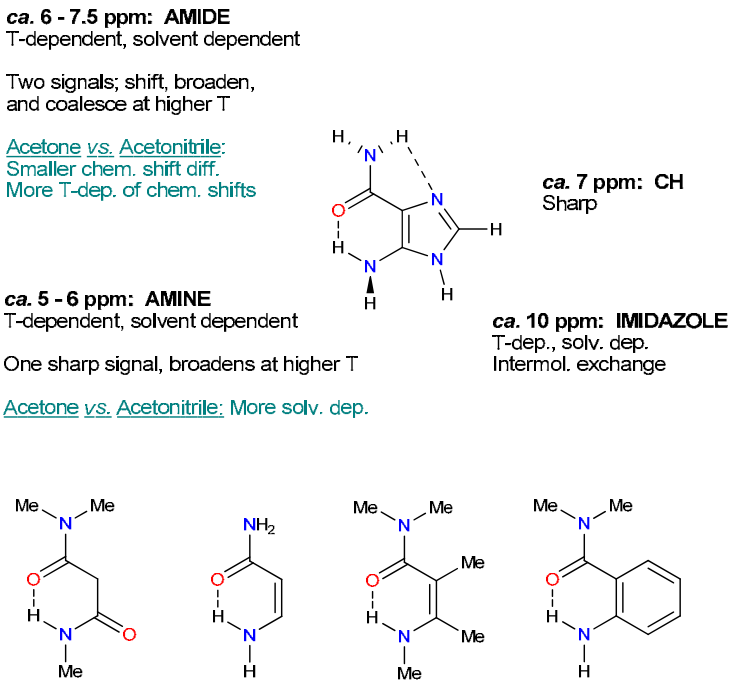

Scheme 4. NMR assignment and intramolecular amino-carbonyl interaction.

The assignment of the spectra to stereoisomer AICA1 is corroborated by studies of intramolecular carbonyl-amino interactions in malonamides and acrylamides. VT-NMR and IR studies by Gellman et al.[19] and the recent electron diffraction and theoretical studies by Belova et al.[20] show malonamide to adopt the six-membered ring structure. In their computational study of conjugated amides, Berg and Bladh reported a *Z*-preference of ΔH_{298} = 3.3 kcal/mol for β-amino-acrylamide, H_2N–CH=CH–$CONH_2$,[21] and Gilli et al. employed the resonance-assisted hydrogen bond (RAHB) rule and the electrostatic-covalent H-bond (ECHBM) model to characterize the intramolecular HB in the pentamethyl derivative shown in Scheme 4.[22] AICA is closely related to *ortho* amino-substituted *N*,*N*-dimethylbenzamide (Scheme 4), and Fong reported a rotational barrier of 14.19 kcal/mol about the C–N bond.[23]

Table 3. Crystal Structures of AICA Derivatives and AICA·L Adducts.

Molecule	Tautomer	Packing Features	Authors	Ref.
AICA nucleoside	AICA1	HB(ribose-OH to imidazole-N)	Adamiak	24
AICA nucleotide	Protonated	zwitterions N-prot. imidazole	Adamiak	24
N1-diphenylmethyl AICA	AICA1	amide dimer, amide-amine to imidazole-N in both ways	Banerjee	24
N1-2-(diethylamino) ethyl AICA	AICA1	stacked amide dimers	Dey	24
N1-(2-hydroxyethyl) AICA	AICA1	HB(amide-NH_2 to alc-O)	Banerjee	27
N1-acetamide AICA	AICA1	stacked columns	Banerjee	27
AICA·C_3H_7OH	AICA1	See text.	Kalman	29
AICA·H_3PO_4	Protonated	ion pair N-prot. AICA and $H_2PO_4^-$	Kalman	29
AICA·H_2O	Tautomer	See text.	Kalman	29

We reviewed the crystallographic record[24-29] (Table 3) and found that all N1-derivatives of AICA as well as the co-crystal formed between the parent AICA and propanol contain the stereoisomer AICA1. However, the crystal structure of AICA·H_2O contains the alternative imidazole tautomer and a closer inspection is warranted (Figure 2). In the crystal structure of AICA·H_2O, one amide-H engages in hydrogen bonding (HB) to water and every water molecule act as donor in one H-bond with an imidazole N-acceptor and another H-bond with an amino-N of an AICA molecule in layer above or below (not shown). The carbonyl acceptor engages in strong bifurcated H-bonding with the second amide-H and the H at N1. All H-donors are engaged and the weakest H-bonding acceptor is left unused, the amide-N. In the propanol co-crystal, one amide-H again engages in H-bonding to water. However, propanol has only one chance to engage in H-bonding as a donor

and does so with the very best H-bond acceptor available, the carbonyl. The amide-N and the imidazole-N of one AICA molecule both engage in H-bonding with the H atoms of the amino group of a neighboring AICA molecule. In the propanol architecture no use is made of the amino-group as acceptor and of second amide-donor.

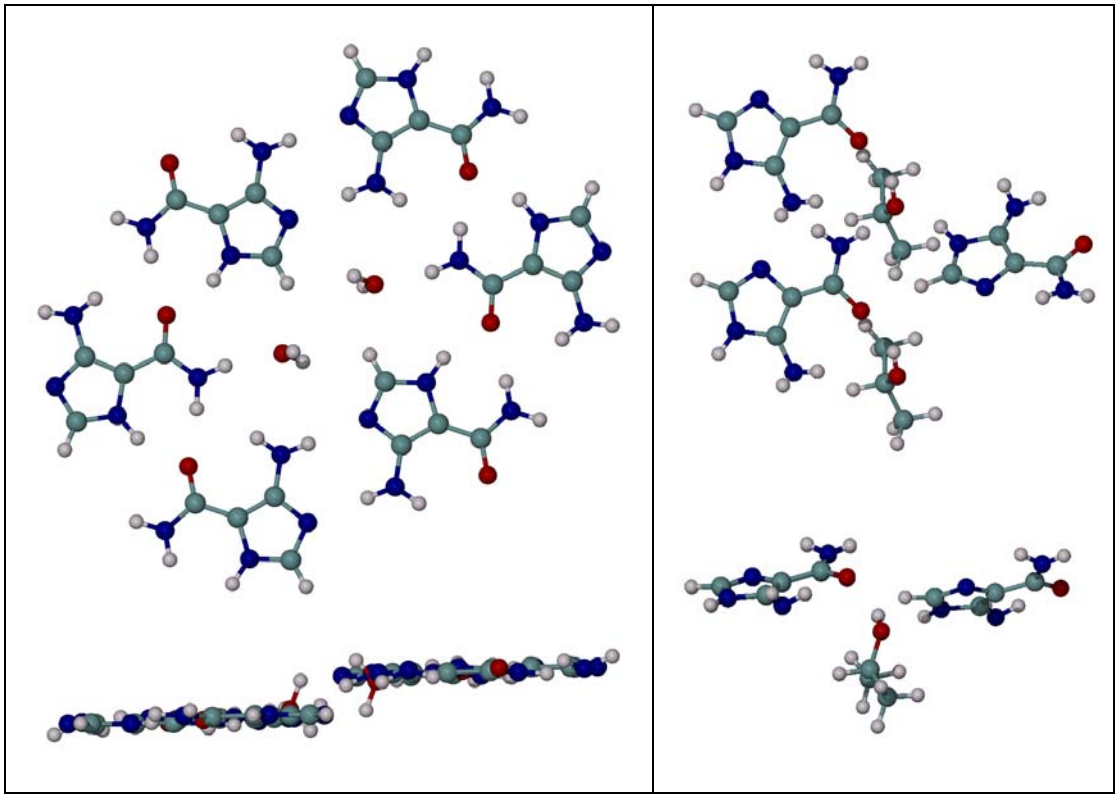

Figure 2. Intermolecular interactions in the crystal structures of AICA·H_2O (left) and AICA·iPrOH. Side-views are provided of the aggregates shown.

The discussion of the crystal packings of the adducts AICA·L shows that a great many intermolecular interactions are in play and this is true for all of the crystal structures of AICA derivatives as well (Table 3). Hence, the crystallographic record does not allow for direct deductions as to the structure of AICA in the liquid or gas phases. Instead, the solid state information is most useful as a resource about structural options that might inform the analysis of solution effects (Scheme 5).

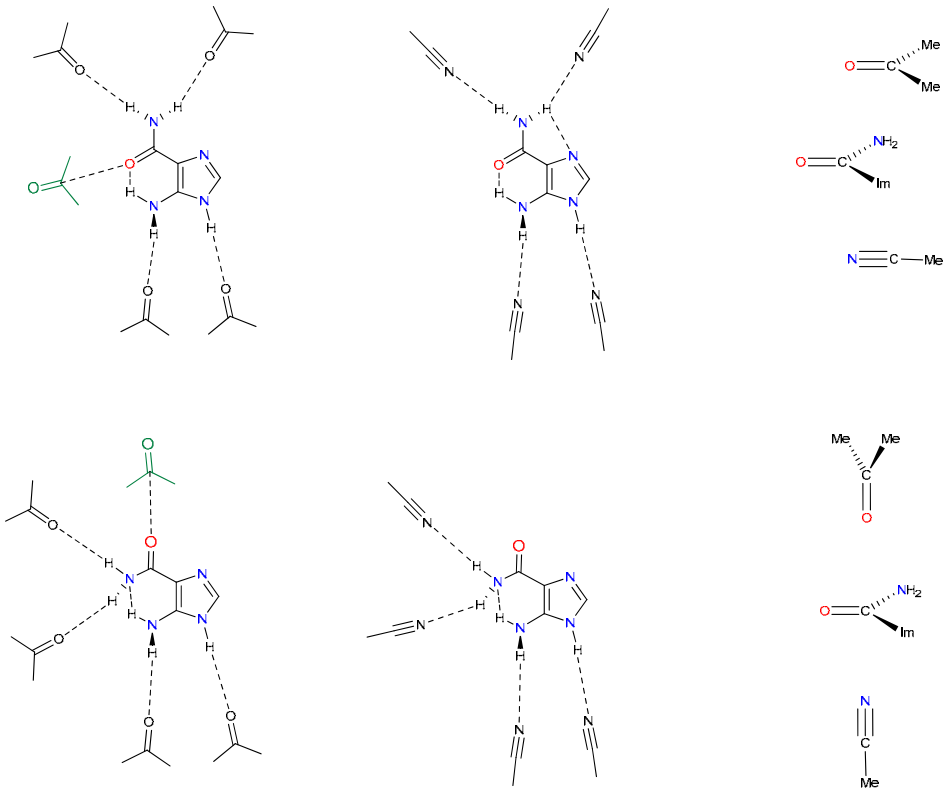

Scheme 5. Intermolecular interactions between AICA and solvents acetone and acetonitrile.

Both solvents can engage HB-donors of AICA1 (top, left and center) and AICA2 (bottom, left and center) more or less in AICA's molecular plane. Both solvents can engage polar bonds of AICA with parallel-offset (top right) and T-shape (bottom right) interactions. In addition, acetone can engage strongly polar bond of AICA by parallel collinear alignment; i.e., green acetone aligned with amide-carbonyl bond.

Acetone[30] and acetonitrile[31] form highly structured liquids because of their large dipole moments (acetone: 2.88 D, acetonitrile: 3.92 D). Acetone and acetonitrile form parallel-offset and T-shaped dimers, respectively, and both solvents can stabilize polar bonds of AICA by association above and below AICA's molecular plane and both parallel or perpendicular to it. In contrast to acetonitrile, acetone allows for attraction via collinear parallel alignment and, hence, acetone can interact with the amide's carbonyl group more or less in the molecular plane (Scheme 5, green solvent molecules). Acetone and acetonitrile both are HB-acceptor solvents without

significant HB-donor ability. One HB-donor of AICA1 is engaged in an intramolecular amino-carbonyl H-bond (NH···OC) and this interaction is steady over time even though the amino group constantly inverts and rotates even at very low temperatures. Thus, four HB-donors are available for interactions of AICA1 with solvent molecules and these interactions are highly flexible in number, geometry, and strength. The scrambling of the amide-H atoms in AICA1 will require some reorganization of solvent molecules engaged in interactions with the amide HB-donors. On the other hand, this scrambling is not expected to cause any significant electronic relaxation and/or changes in solvation in the remainder of the molecule. And yet, the spectra in Figure 1 show pronounced broadening of the amino group signal and a shift to lower chemical shifts with increasing temperature in both solvents, and these T-dependent effects are more pronounced in acetone. These features are inconsistent with and therefore deny the interpretation of the VT-NMR data as the result of amide-H scrambling by simple amide NH_2 rotation in one stereoisomer.

3.2 Potential Energy Surface Analysis

This theoretical method is to explore the possibility of amide protons exchanging through isomerism and investigate dynamic NMR events of AICA compounds in different solvents, e.g., acetone or acetonitrile, from a theoretical point of view. Potential energy surface analysis has proven to be of assistance to interpret these experimental findings and gain deeper structural and dynamic insights. In our current study, all possible conformers of AICA (Scheme 2) have been taken into account to be responsible for NMR dynamics. Since the publication of this work, theoretical studies for AICA and its analogues are scarce in the literature, and several are found below. Shim and coworkers[32] proposed model system of AICA and formamide to confirm proton-shuttling mechanism of AICAr Tfase assisted by 4-carboximide group. Qiao et al.[33] also employed AICA and M-AICA (N-Methyl AICA) to model molecule AICAR, thereby evaluating catalytic mechanism of AICAR

Transformylase. In these papers, ribose moiety in AICAR was replaced by a hydrogen atom or a methyl group so as to simplify the molecules of interest in each case, thus saving time and cost without significant loss of good accuracy. There are relatively few conformational analyses of AICA and its derivatives discussed in quantum chemical calculation. However, this information gives us little help to explain our case. As a result, a more detailed electronic structural examination for AICA should be systematically undertaken in our study.

Structural Analysis of Minima. Molecular model about all possible AICA conformers and isomers are demonstrated in Figure 3, in ball-stick form.

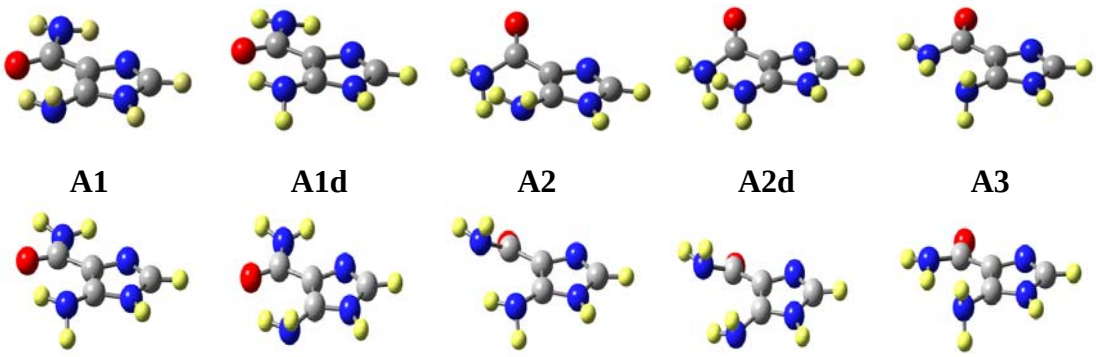

Figure 3. MP2(full)/6-311++G** optimized stationary structures for AICA.

As can be seen, the major geometrical difference between **A1** type and two other types **A2**, **A3**, lies in the orientation of carbonyl C=O in the carboxamide $CONH_2$ group. The carbonyl oxygen in **A1** is pointed toward the 5-amino NH_2 group and cis to C4=C5 of imidazole ring with respect to single bond of C4—CO; while in **A2** and **A3**, it is actually trans to the ring C4=C5 and carboxamide NH_2 is oriented to the 5-amino group. Although **A2** and **A3** are very similar since the 4-carboxamide group is situated in almost same way, each of protons in 5-amino group of **A3** does not lie in the ring plane, nearly symmetrized to each other in terms of imidazole ring plane. That's also the reason why AICA3 diastereomers were not found on

exploration of potential energy surface.

The selected geometrical parameters, including the bond lengths, angles and dihedral angels, have been reported in Table 4 and Table 5.

Table 4. Selected Geometrical Parameters of AICA Isomers at MP2 Level.[a]

Geometry Parameters	**A1**	**A1d**	**A2**	**A2d**	**A3**
Bond Length (Å)					
C4C5	1.386	1.386	1.392	1.392	1.391
C4C6	1.467	1.467	1.474	1.479	1.492
C5N9	1.389	1.389	1.400	1.402	1.412
C6O7	1.234	1.234	1.217	1.217	1.222
C6N8	1.364	1.363	1.403	1.400	1.376
N9H12	1.018	1.018	1.015	1.014	1.015
Bond Angle (deg.)					
C4C5N9	131.63	131.49	133.51	134.22	130.48
C5C4C6	124.84	124.85	126.71	127.65	128.83
C4C6O7	121.64	121.65	124.56	123.89	122.30
C4C6N8	114.62	114.66	112.80	113.61	114.32
C6N8H10	117.06	117.26	114.72	115.07	118.04
C6N8H11	117.76	117.99	112.40	112.49	115.14
C5N9H12	108.64	108.58	110.08	110.35	112.81
C5N9H13	113.56	113.54	112.42	113.12	112.76
Dihedral (deg.)					
C5C4C6O7	-6.18	0.59	145.06	146.16	169.46
C5C4C6N8	171.61	178.64	-31.13	-30.14	-13.03
C4C6N8H10	166.96	167.86	-42.20	-39.58	19.70
C4C6N8H11	14.60	14.00	-173.27	-171.71	167.29
C4C5N9H12	-5.47	8.26	-9.70	-5.96	114.96
C4C5N9H13	-128.95	131.58	-131.73	116.86	-120.15

Table 5. Bond Lengths for Possible Hydrogen Bonds in AICA Molecules.

H-Bond (Å)	**A1**	**A1d**	**A2**	**A2d**	**A3**
O7···H12	2.198	2.196	−	−	−
N3···H11	2.399	2.402	−	−	−
N8···H12	−	−	2.350	2.495	−
N9···H10	−	−	−	−	2.145

We can see dihedral angle data for amide Hs in Table 4, for all of AICA conformations, no one is close to 0° or 180°, suggesting that they are not planar, mostly owing to avoidance of steric effect and intramolecular repulsion.

Two major possible intramolecular H-bonds are shown in Scheme 2 and Table 5. One is N-H···O=C, the other is N-H···N. The existence of these non covalent bondings in the molecule results in the structural distinction and geometrical preference between AICA1 and AICA2 or AICA3. In **A1** and **A1d**, the distance of O7···H12 are 2.198 and 2.196 Å. They are both typical indicatives of formation of strong H-bond. In addition, the bond lengths of N3···H11 in AICA1 analogs are 2.399 and 2.402, which are much longer and correspond to a relatively weaker interaction. While in **A2**, **A2d** and **A3**, there is only one H-bonding in their molecules. It is clear that they belong to same kind of H-bonds, but the H-bond donor nitrogen atom came from different groups. And the distance ordering is **A3** < **A2** < **A2d.** As a consequence, hydrogen bond strength of **A3** is biggest one among them, and second to **A2**, the last is **A2d**.

Isomer Preferences. Relative energies and activation barriers for isomerizations of conformers of AICA are reported in Table 6 in gas phase and Table 7 considering bulk solvents.

Table 6. Relative Energies and Activation Barriers for AICA in Gas-Phase[a]

Parameter	ΔE	ΔH_0	ΔH_{298}	ΔG_{298}
E_{rel}(**A1d** *vs.* **A1**)	0.11	0.07	0.09	0.12
E_{act}(**A1**,**RTS1(A1,A1d')**)	18.82	17.97	17.71	18.11
E_{act}(**A1d'**,**RTS1(A1,A1d')**)	18.71	17.90	17.62	17.99
E_{act}(**A1**,**RTS2(A1,A1d')**)	17.30	16.49	16.24	16.61
E_{act}(**A1d'**,**RTS2(A1,A1d')**)	17.19	16.41	16.15	16.49
E_{act}(**A1**,**ITS(A1,A1d')**)	0.28	-0.41	-0.55	-0.37
E_{act}(**A1d'**,**ITS(A1,A1d')**)	0.18	-0.48	-0.64	-0.49
E_{act}(**A1**,**ITS(A1,A1d)**)	3.00	1.61	1.73	1.35
E_{act}(**A1d**,**ITS(A1,A1d)**)	2.89	1.53	1.63	1.23
E_{act}(**A1**,**RTS1(A1,A1d)**)	2.21	1.90	1.63	1.91
E_{act}(**A1d**,**RTS1(A1,A1d)**)	2.10	1.83	1.54	1.79
E_{act}(**A1**,**RTS2(A1,A1d)**)	9.48	8.67	8.49	8.53
E_{act}(**A1d**,**RTS2(A1,A1d)**)	9.37	8.59	8.39	8.41
E_{rel}(**A2d** *vs.* **A2**)	0.70	0.61	0.68	0.51
E_{rel}(**A2** *vs.* **A1**)	10.01	10.00	9.98	9.86
E_{rel}(**A2d** *vs.* **A1**)	10.71	10.61	10.65	10.37
E_{act}(**A2**,**RTS(A2,A2d')**)	7.57	6.90	6.55	7.40
E_{act}(**A2d'**,**RTS(A2,A2d')**)	6.86	6.29	5.87	6.90
E_{act}(**A2**,**ITS(A2,A2d)**)	3.38	2.29	2.36	1.72
E_{act}(**A2d**,**ITS(A2,A2d)**)	2.68	1.68	1.68	1.21
E_{act}(**A2**,**RTS(A2,A2d)**)	1.51	1.22	0.95	1.23
E_{act}(**A2d**,**RTS(A2,A2d)**)	0.81	0.62	0.27	0.72
E_{rel}(**A3** *vs.* **A1**)	10.63	10.42	10.45	10.07
E_{act}(**A3**,**ITS(A3,A3')**)	0.39	-0.47	-0.57	-0.76
E_{act}(**A3**,**RTS(A3,A3')**)	18.02	16.93	16.87	16.67
E_{act}(**A1**,**CC-RTS(A1,A2')**)	11.86	11.58	11.30	11.55
E_{act}(**A2'**,**CC-RTS(A1,A2')**)	1.85	1.67	1.32	1.69
E_{act}(**A1**,**CC-RTS(A1,A3')**)	14.96	14.12	13.99	14.25
E_{act}(**A3'**,**CC-RTS(A1,A3')**)	4.33	3.70	3.54	4.17
E_{act}(**A2d**,**RTS(A2d,A3')**)	4.51	3.80	3.62	3.54
E_{act}(**A3'**,**RTS(A2d,A3')**)	4.59	3.99	3.82	3.84
E_{act}(**A2**,**RTS(A2,A3')**)	1.31	0.80	0.50	1.24
E_{act}(**A3'**,**RTS(A2,A3')**)	0.68	0.38	0.02	1.02
E_{act}(**A1**,**RTS(A2,A2d')**)	17.57	16.90	16.53	17.26
E_{act}(**A1d'**,**RTS(A2,A2d')**)	17.47	16.83	16.44	17.14

[a] All data computed at MP2(full)/6-311++G**.

Table 7. Relative Energies and Activation Barriers for AICA Considering Bulk Solvation.[a]

Parameter	ΔE_{SP}	ΔE	ΔH_0	ΔH_{298}	ΔG_{298}
In Acetone					
E_{rel}(**A1** *vs.* **A1d**)	-0.02	-0.01	0.17	0.04	0.87
E_{act}(**A1**,**RTS1(A1,A1d')**)	16.22	16.28	15.79	15.32	16.79
E_{act}(**A1d'**,**RTS1(A1,A1d')**)	16.24	16.28	15.62	15.28	15.92
E_{act}(**A1**,**RTS2(A1,A1d')**)	15.21	15.19	14.71	14.28	15.63
E_{act}(**A1d'**,**RTS2(A1,A1d')**)	15.23	15.19	14.54	14.24	14.76
E_{rel}(**A2d** *vs.* **A2**)	0.80	1.05	1.08	1.08	1.15
E_{rel}(**A1** *vs.* **A2**)	5.18	4.56	4.80	4.68	5.28
E_{rel}(**A1** *vs.* **A2d**)	5.98	5.61	5.88	5.76	6.44
E_{act}(**A1**,**CC-RTS(A1,A2')**)	8.87	8.61	8.23	7.94	8.68
E_{act}(**A2'**,**CC-RTS(A1,A2')**)	3.69	4.05	3.43	3.26	3.40
E_{act}(**A2**,**RTS(A2,A2d')**)	6.35	10.00	9.51	9.06	10.15
E_{act}(**A2d'**,**RTS(A2,A2d')**)	8.55	8.95	8.44	7.99	9.00
E_{act}(**A1**,**RTS(A2,A2d')**)	14.53	14.56	14.32	13.74	15.43
E_{act}(**A1d'**,**RTS(A2,A2d')**)	14.55	14.57	14.15	13.70	14.57
In Acetonitrile					
Erel(**A1** *vs.* **A1d**)	-0.04	0.00	0.05	0.03	0.07
E_{act}(**A1**,**RTS1(A1,A1d')**)	16.05	16.14	15.54	15.17	15.86
E_{act}(**A1d**,**RTS1(A1,A1d')**)	16.09	16.14	15.49	15.15	15.79
E_{act}(**A1**,**RTS2(A1,A1d')**)	15.09	15.09	14.49	14.17	14.74
E_{act}(**A1d**,**RTS2(A1,A1d')**)	15.12	15.10	14.45	14.14	14.67
E_{rel}(**A2d** *vs.* **A2**)	0.79	1.04	1.06	1.06	1.16
E_{rel}(**A1** *vs.* **A2**)	4.90	4.25	4.35	4.35	4.12
E_{rel}(**A1** *vs.* **A2d**)	5.73	5.29	5.37	5.39	5.21
E_{act}(**A1**,**CC-RTS(A1,A2')**)	8.69	8.40	7.87	7.69	7.72
E_{act}(**A2**,**CC-RTS(A1,A2')**)	3.78	4.14	3.51	3.34	3.60
E_{act}(**A2**,**RTS(A2,A2d')**)	9.46	10.17	9.70	9.25	10.39
E_{act}(**A2d'**,**RTS(A2,A2d')**)	8.67	9.14	8.64	8.18	9.23
E_{act}(**A1**,**RTS(A2,A2d')**)	14.36	14.43	14.06	13.60	14.51
E_{act}(**A1d'**,**RTS(A2,A2d')**)	14.40	14.43	14.01	13.57	14.44

[a] The ΔE_{SP} data are determined considering solvent by PCM theory based on the same level gas-phase structures; PCM(MP2(full)/6-311++G**)//MP2 (full)/ 6-311++G**. All other data are based on PCM theory with structure optimization and vibrational analysis at the PCM level; PCM(MP2(full)/6-311++G**) :=

PCM(MP2(full)/6-311++G**)//PCM(MP2(full)/6-311++G**).

In above tables, we found that there are two model systems: AICA1 and AICA1-dia, are most stable and almost similar in energy. Particularly, **A1** is the most stable AICA conformation in gas phase, followed by **A1d**, then **A2** and **A3**, and **A2d** is the least stable one, which is c.a. 10.71 kcal/mol higher than **A1**. Moreover, isomer **A2d** is preferred over **A2** by ΔE = 0.70 kcal/mol. In aqueous phase, same law applies to most cases noted before. The only exception is that **A1d** is more negative in energy compared with **A1,** but with little difference in value. They could coexist at same proportion.

Rotational Isomerization of AICA1 Isomers. As Figure 4 illustrates, when amide hydrogens on carboxamide group in AICA1 rotate about CO-N bond, AICA1 will finally turn into AICA-dia'. The activation barriers to fall into **A1d'** from **A1** via RTS1(**A1,A1d'**) and RTS2(**A1,A1d'**) are 18.11 kcal/mol and 16.61 kcal/mol, respectively. They are relatively high in energy, but when considering solvation, barriers for these two rotational pathways significantly decrease a lot. 16.79 kcal/mol and 15.63 kcal/mol are calculated in acetone, and 15.86 kcal/mol and 14.74 kcal/mol in acetonitrile. It demonstrates that these polar solvents interacting with AICA solutes are favorable to such diastereoisomerization. On the other hand, if amino group rotates around imidazole-ring C-N bond, AICA1 goes to AICA1-dia. Compared to amide rotation, amino rotation is relatively easily accessible and activation barriers through RTS1(**A1,A1d**) and RTS2(**A1,A1d**) are 2.21 kcal/mol and 9.48 kcal/mol in gas phase, respectively. We also found barriers in acetonitrile are dropping more than those in acetone. It also shows that enantiomerization between **A1** and **A1'** can not occur via simple conversion unless two amino rotational pathways proceed simultaneously or stepwise.

Figure 4. Enantiomerization and Diastereoisomerization of **AICA1** and **AICA1-dia** by amino-rotation.

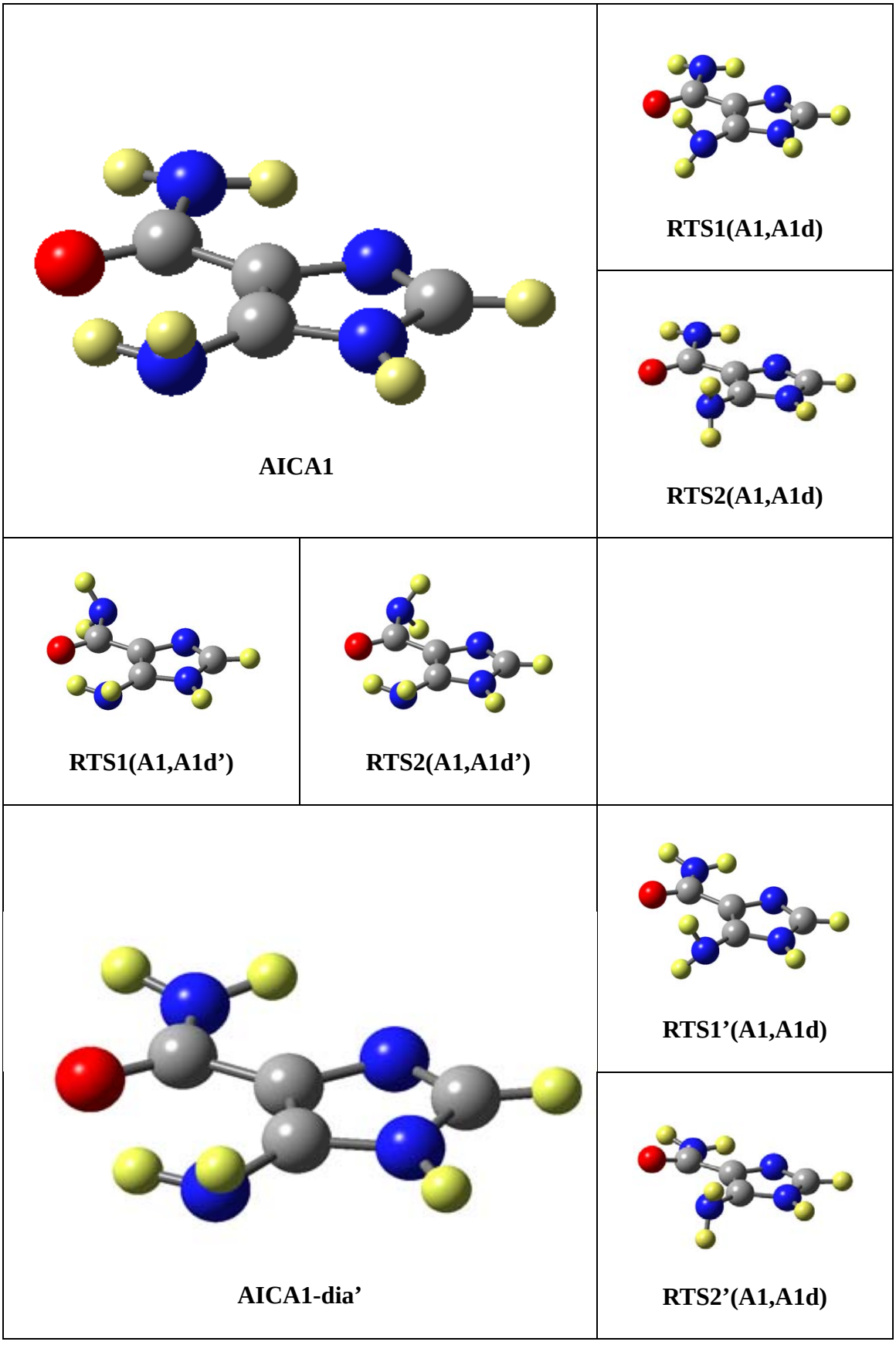

Figure 4. (Continued. Attach to the right.)

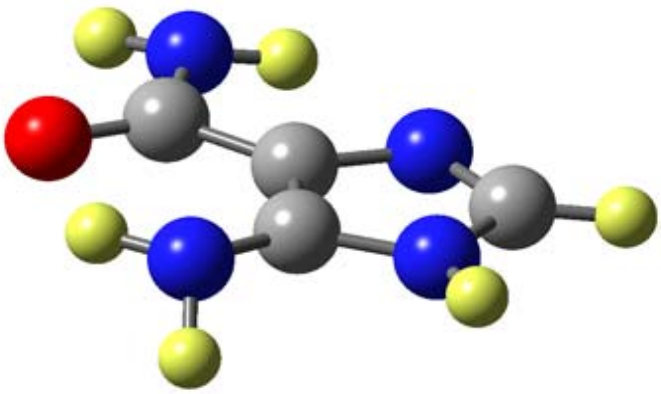

AICA1-dia

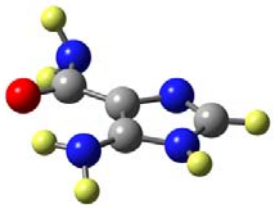

RTS1'(A1,A1d')

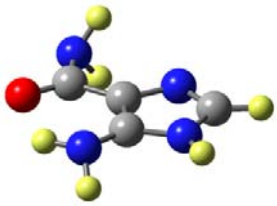

RTS2'(A1,A1d')

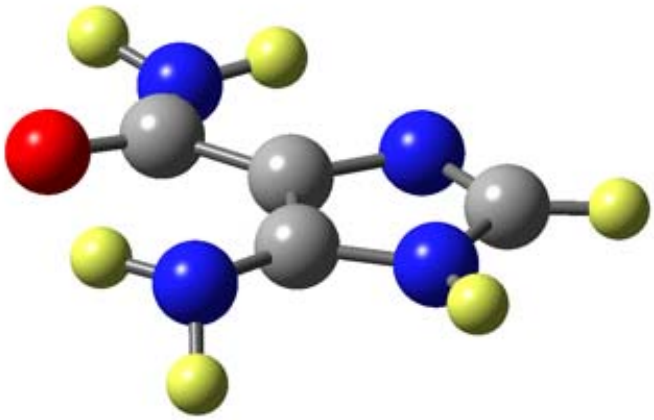

AICA1'

Figure 5. Enantiomerization and Diastereoisomerization of **AICA1** and **AICA1-dia**, respectively, by N-Inversion.

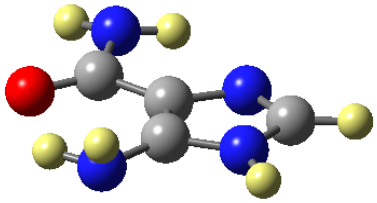 **AICA1**	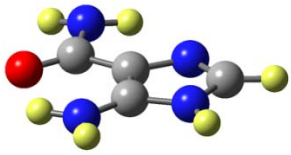 **ITS(A1,A1d)**	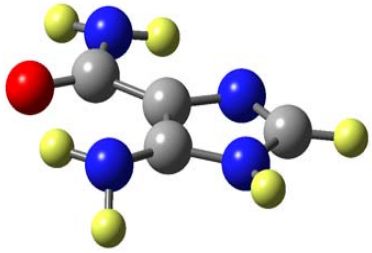 **AICA1-dia**
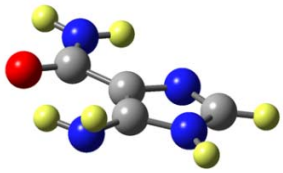 **ITS(A1,A1d')**		 **ITS'(A1,A1d')**
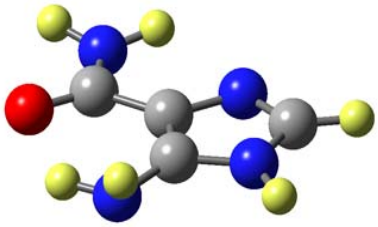 **AICA1-dia'**	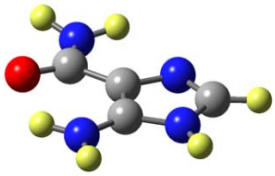 **ITS'(A1,A1d)**	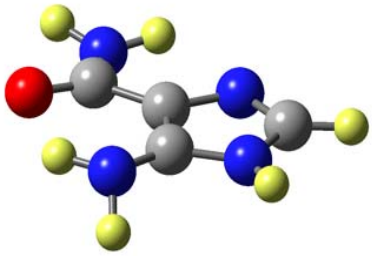 **AICA1'**

Figure 6. 3D PES (left and right side view).

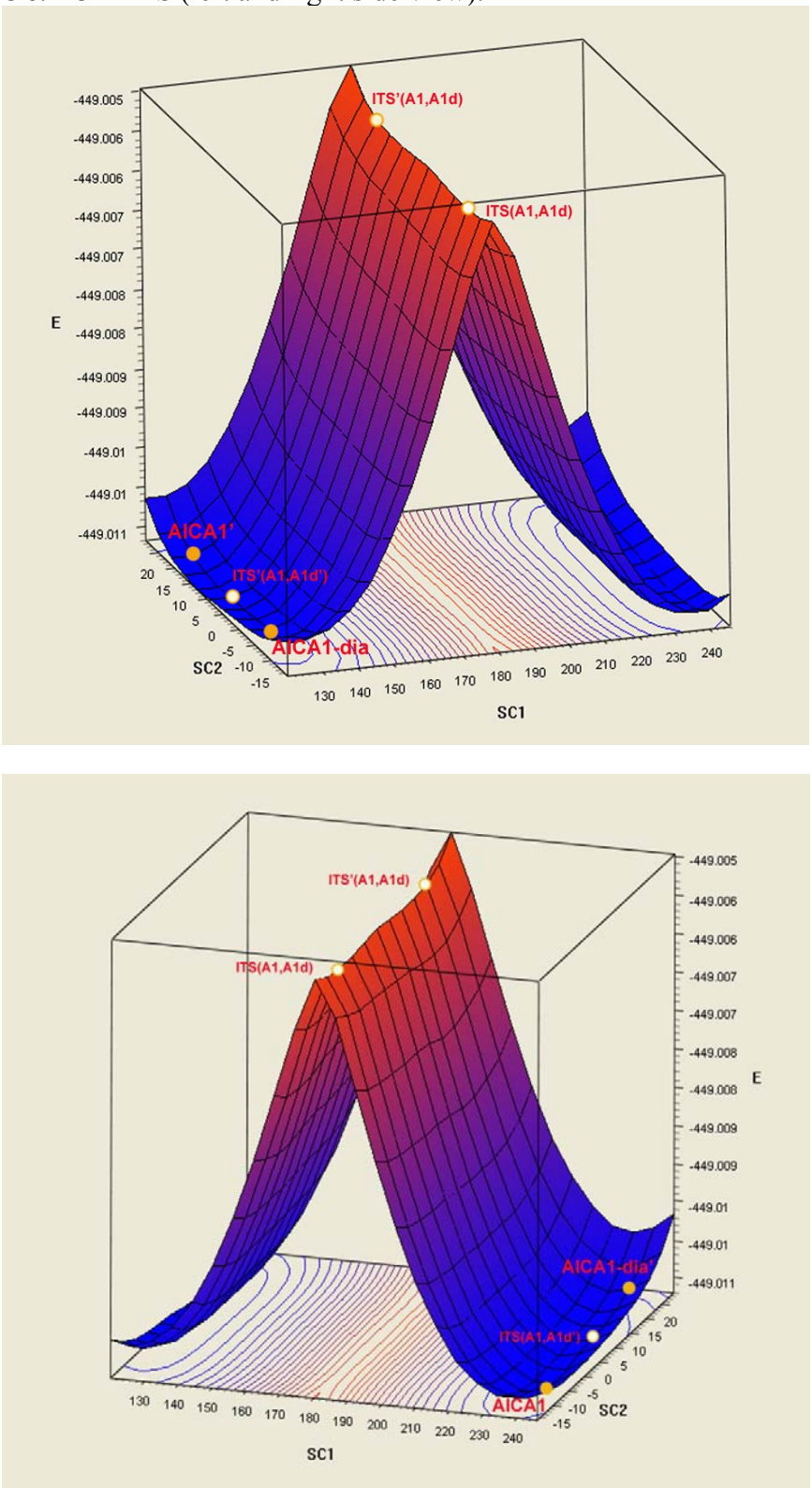

Inversional Isomerization of AICA1 Isomers. Starting from AICA1 structures, we also searched four amino-inversional transition states in **A1** and **A1d** systems. Their structures are shown in Figure 5, and graphic inversional pathways are illustrated in Figure 6 (3D PES). Seen from both figures, the barriers corresponding to amino inversion are relatively high on curves, c.a. 1.35 kcal/mol for **A1** to isomerize to **A1d**. Howver, it seems that amide inversion **TSs** on 3D surface are pretty much similar to minima in energy. Furthermore, the computed Gibbs free energies for these processes are incredibly negative. It suggests three possibilities: first, the inversion course via ITS(**A1,A1d'**) is able to take place spontaneously; second, ITS(**A1,A1d'**) is not transition state at all; third, the computational methods we used can not apply to inversion case. In separate paper, the results obtained by corrected quantum method and anharmonic vibrational analysis will shed some light on this problem.

Isomerization of AICA2 Isomers. For AICA2 to AICA2-dia, shown in Figure 7, they can undergo through dissimilar rotational and inversional transition states. The formation of **A2d** via nearly planar transition state ITS(**A2,A2d**) reveals readily attained pathway to such diastereoisomerization ($\Delta G_{act} < 1.72$ kcal/mol). In addition, the conversion between **A2** and **A2d** by aid of transition RTS(**A2,A2d**) is much easier to occur due to even smaller activation barrier ($\Delta G_{act} < 1.23$ kcal/mol). To large extent, they are both able to happen and are competing in the process. Interestingly, unlike AICA conformers, the analogous amide-inversion TS has not been found yet on PES. But multiple rotational transition state was accidentally being located during the operation of looking for ITS. It provides likelihood that interconversion between **A2** and **A2d'**. Another important pathway via RTS(**A2,A2d'**) that might be responsible for amide protons scrambling in NMR dynamics is listed in Figure 7 as well. The activation barrier in junction with this passage is relatively high ($\Delta G_{act} > 9.23$ kcal/mol), thus providing an alternative to reasonably interpret our NMR data.

Figure 7. Enantiomerization and Diastereoisomerization of **AICA2** and **AICA2-dia** by amino-rotation snd -inversion.

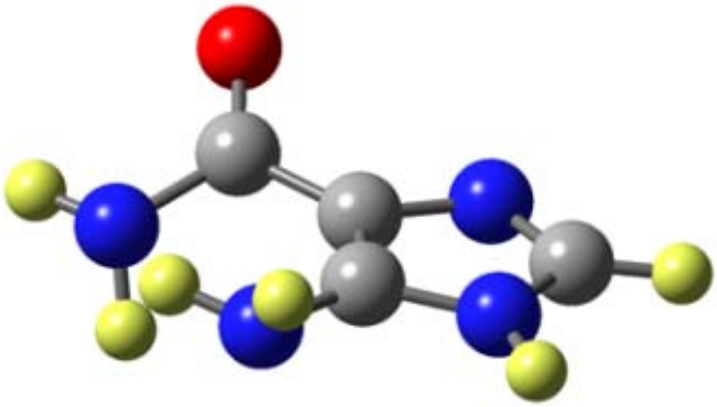

AICA2

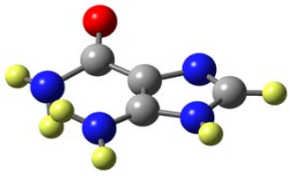

ITS(A2,A2d)

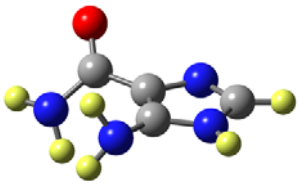

RTS(A2,A2d)

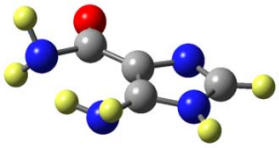

RTS(A2,A2d')

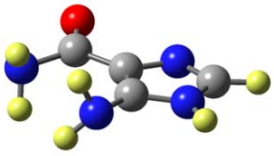

MPTSR-TS

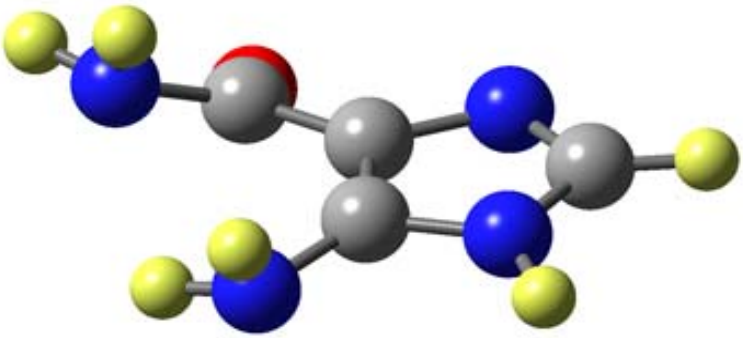

AICA2-dia'

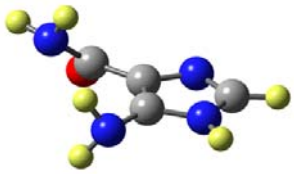

RTS'(A2,A2d)

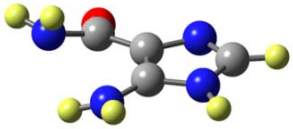

ITS'(A2,A2d)

Figure 7. (Continued. Attach to the right.)

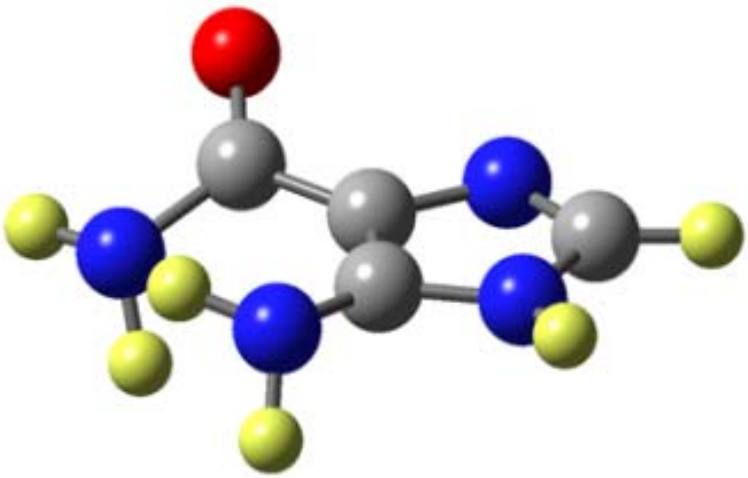

AICA2-dia

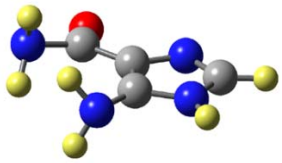

MPTSR-TS'

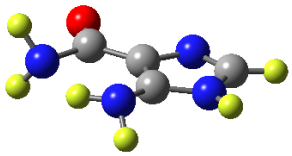

RTS'(A2,A2d')

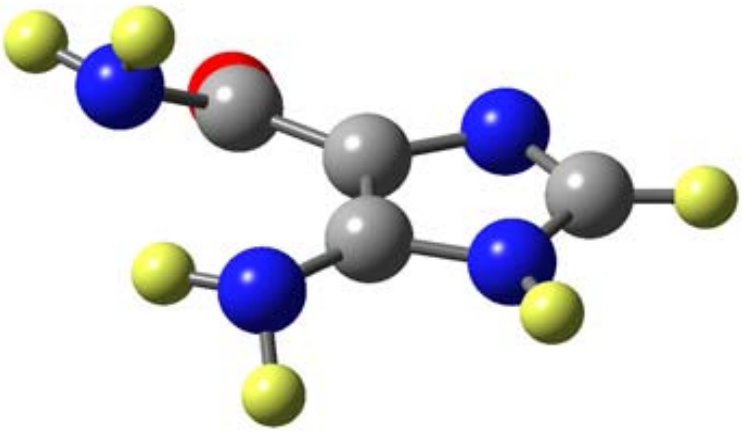

AICA2'

Figure 8. Enantiomerization of **AICA3** by N-inversion or amio-rotation.

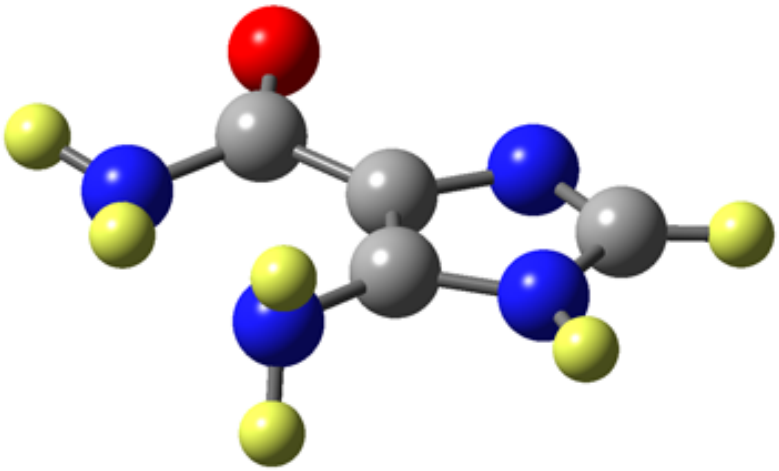

AICA3

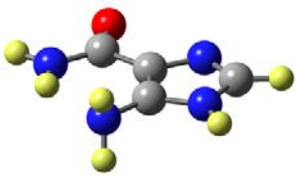

ITS(A3,A3')

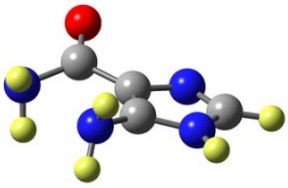

RTS(A3,A3')

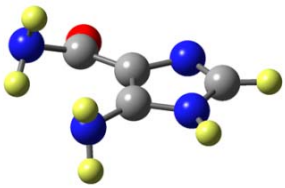

RTS'(A3,A3')

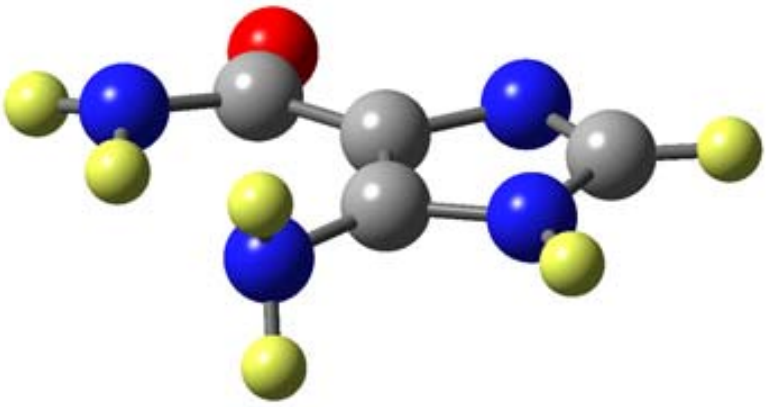

AICA3'

Enantiomerizations of AICA3. As illustrated in Figure 8, with AICA3 amino group remaining almost the same way, amide group may invert or rotate to yield three transition structures ITS(**A3, A3'**), RTS(**A3, A3'**) and its mirror state RTS'(**A3, A3'**). The barrier is extremely high (ΔG_{act} = 16.67 kcal/mol) for rotation, and very low (ΔG_{act} = -0.76 kcal/mol) for inversion. They are both similar to AICA1 case.

Diastereoisomerization of AICA2 to AICA3. By rotating imidazole C-NH_2 bond, AICA2 conformers can isomerize to AICA3 or AICA3'. These pathways are illustrated in the central column of Figure 9. The alternative rotational isomerization of **A2** and **A3** was constructed as a series of constrained optimization keeping CCNH torsion angle (α) at fixed values. The resulting potential energy curves were plotted in Figure 10.

In the case of **A2,** we see that as the dihedral angle α approached c.a. ±70°, two energy maxima have been located and confirmed as two distinctive rotational **TS**s, RTS(**A2,A2d**) and RTS(**A2,A3'**). The barriers with respect to these states are 1~1.5 kcal/mol. This value is not that big, and isomers **A2** and **A3** can interchange much easily. Continuing to increase or decrease angle α in opposite direction, equilibrium structures **A2d** near 120° and **A3** corresponding to c.a. -120° are observed. Along right rotational path from **A2d**, relatively higher barrier (3.54 kcal/mol) stemming from transition state RTS(**A2d,A3'**) around 180°, has to be overcome to yield **A3'**. Same rule and passage could be employed to describe another pure rotational pathway: **A3 → A2' → A2d'**. In fact, the first route and second are just two mirror processes, having enatio counterparts with identical energy. Low barrier of invisional paths for **A3** and **A3'** make them interconnected to each other.

Figure 9. Diastereoisomerization of **A1**, **A2** and **A3** by carboxamide rotation.

		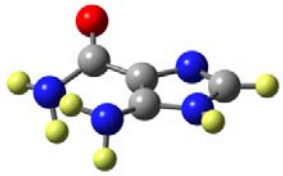 **AICA2-dia**	<===>
		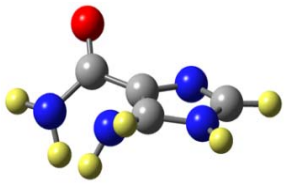 **RTS(A2d,A3')**	
 **AICA1**	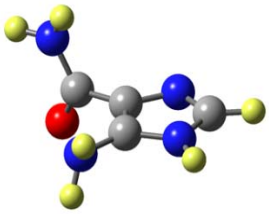 **CC-RTS(A1,A3')**	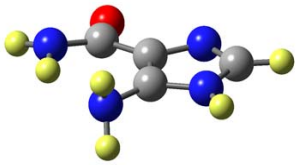 **AICA3'**	<===>
		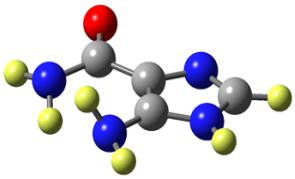 **RTS(A2,A3')**	
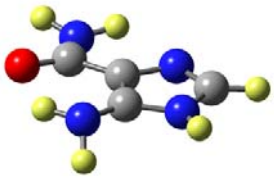 **AICA1'**	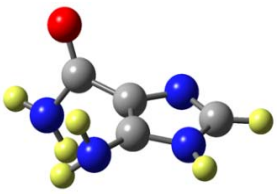 **CC-RTS(A1',A2)**	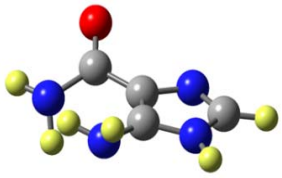 **AICA2**	<===>

Figure 9. (attach to right)

<===>	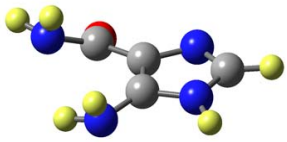 **AICA2-dia'**		
	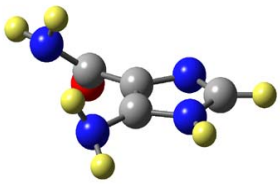 **RTS'(A2d,A3')**		
<===>	 **AICA3**	 **CC-RTS'(A1,A3')**	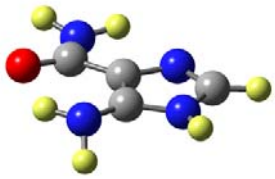 **AICA1'**
	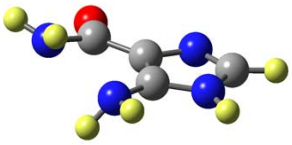 **RTS'(A2,A3')**		
<===>	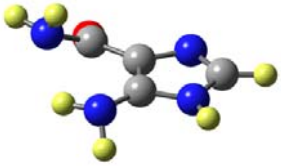 **AICA2'**	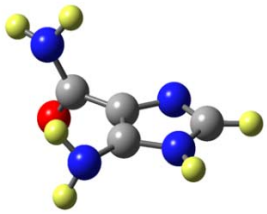 **CC-RTS'(A1',A2)**	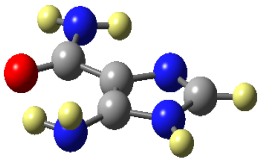 **AICA1**

Figure 10. Computed Discretized Rotational Energy Profiles of **AICA**. The profiles for the amino group rotations are shown as a function of the ∠(C4=C5–N–H) dihedral angle α..

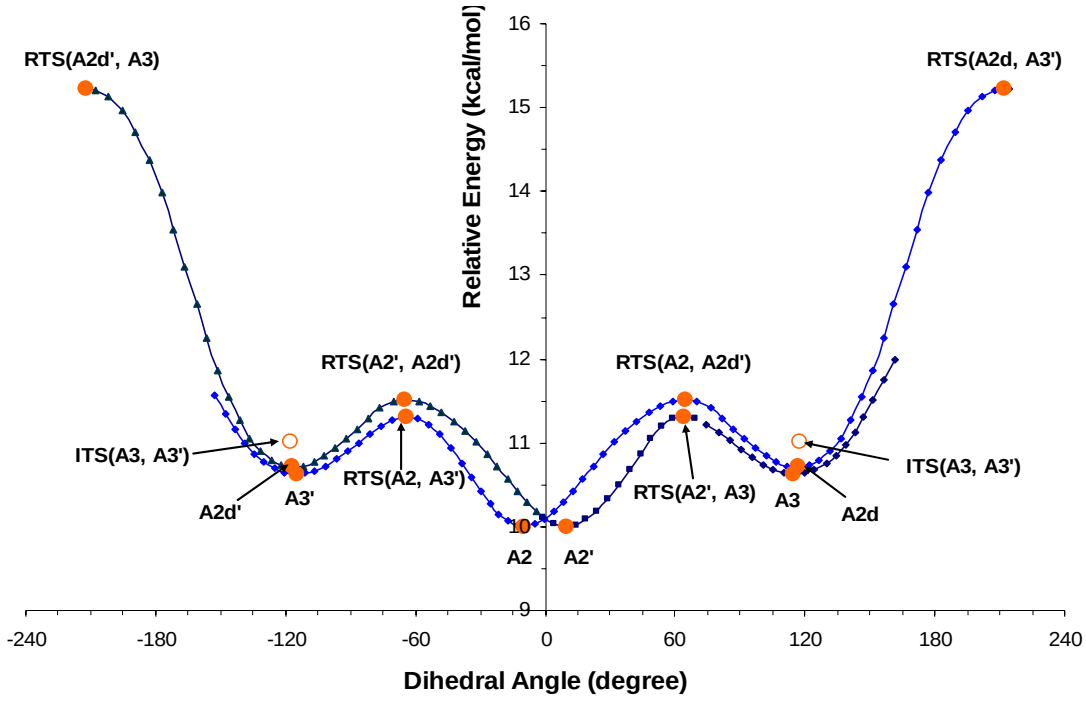

Figure 11. Computed Discretized Rotational Energy Profiles of **AICA**. The profiles are shown as a function of the ∠(C5=C4–C=O) dihedral angle ω. An overview is provided in part (a), and parts (b) and (c) show two pertinent regions with doubled vertical resolution.

(a)

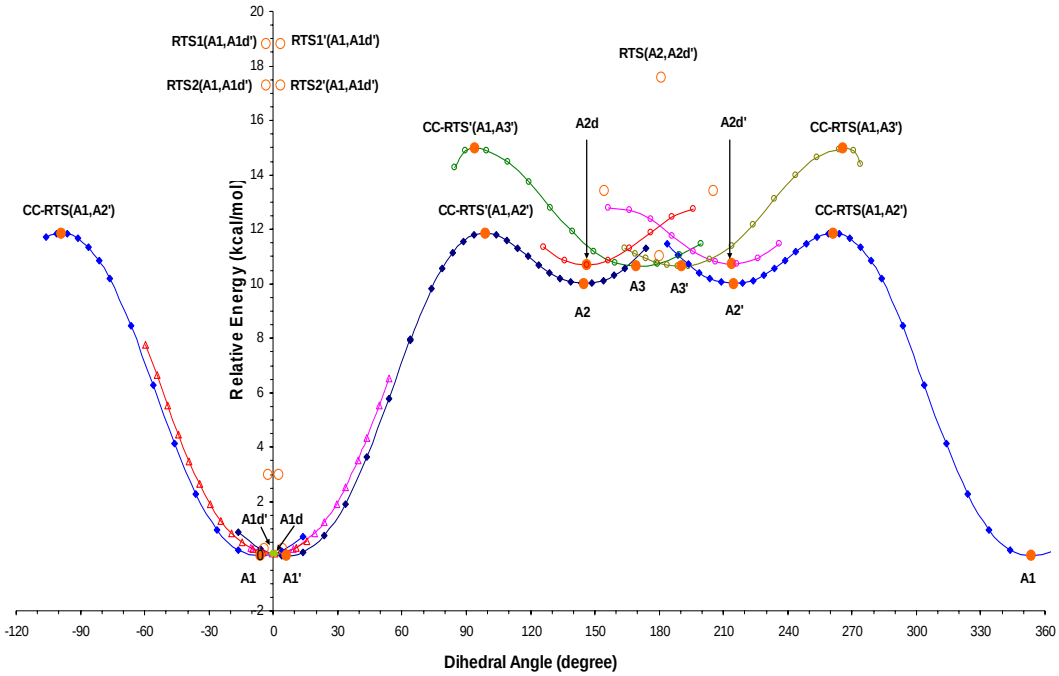

(b) and (c)

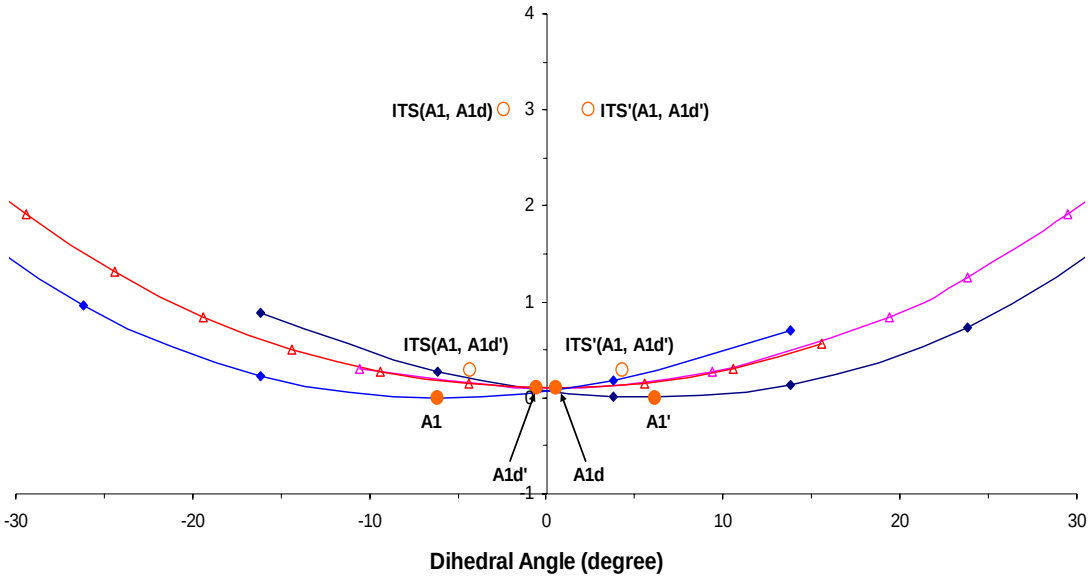
ITS(A1, A1d)
ITS'(A1, A1d')
ITS(A1, A1d')
ITS'(A1, A1d')
A1
A1'
A1d'
A1d
Dihedral Angle (degree)

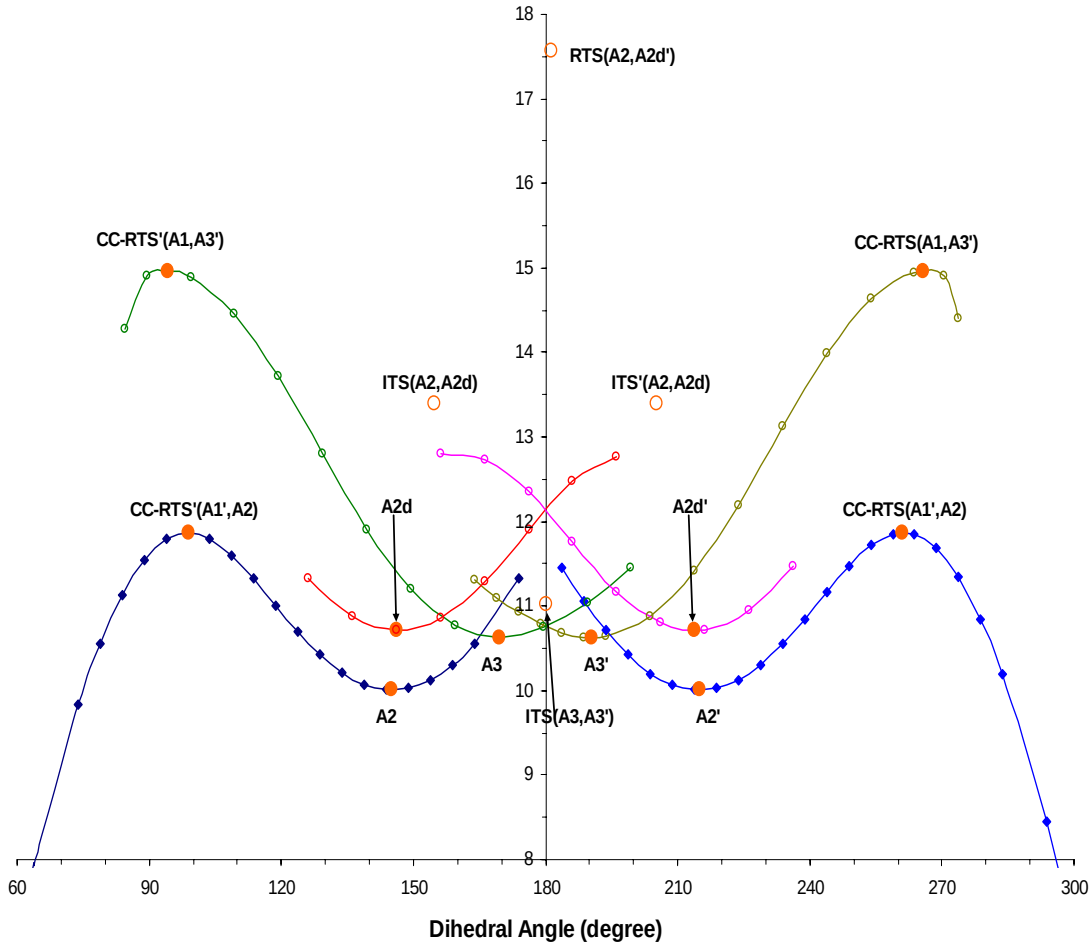
RTS(A2,A2d')
CC-RTS'(A1,A3')
CC-RTS(A1,A3')
ITS(A2,A2d)
ITS'(A2,A2d)
CC-RTS'(A1',A2)
A2d
A2d'
CC-RTS(A1',A2)
A3
A3'
A2
ITS(A3,A3')
A2'
Dihedral Angle (degree)

Diastereoisomerization of AICA1 to AICA2 or AICA3. In the past, a large amount of aromatic amides have been explored, especially for isomerization accounted for all of Ar-CO rotations. This is due to importantance of them regarded as atropisomeric molecules. These restricted rotational compounds are powerful controllers of stereoselectivity and used as chiral auxiliaries in organic synthesis. [34] They can exist as enantiomers at room temperature if such rotation is very slow, i.e., Ar-CO rotational barrier is high enough (>21 kcal/mol).[35].

Although AICA is also aromatic amides whose imidazole ring is a planar 6π-aromatic heterocycle, it has a low barrier $\Delta G_{act.}$< 15 kcal/mol due to unsubstitution of amide and can not be atropsomeric at ambient temperature. However, if temperature is decreasing to some degree, the rate of rotation about Ar-CO will be slow, and then rotamers interconvert not fast, their diastereomers might be able to appear. So in this section, our focused target is exocyclic single bond Ar-CO rotation and its role in the isomerization of AICA molecules. So far, there is no paper to investigate this aspect, although large amount of aromatic amides have been studied to determine barriers to rotation about the aryl-carbonyl bond by aid of VT NMR spectroscopy.

Since proteins and polypeptides contain peptide bonds (-CONH-) and nucleobases have quite a few aromatic ring nitrogens, and they are both play critical role in the life activities by means of hydrogen bonding, [36] it could be of great interest to make AICA molecules as building blocks in proteins and enzymes and combine NMR technique with theoretical analysis to study their dynamics in solution.

Computations on Ar-CO bond rotation render four possible pathways for interconversion between **A1**, **A2** and **A3** rotamers, shown in two horizontal columns of Figure 9: **A1** → CC-RTS**(A1,A3')** → **A3', A1** → CC-RTS**(A1,A2')** → **A2',** and their prime processes. The barriers for CC-rotation **A1** → **A3'** and **A1** → **A2'** are 14.25 kcal/mol and 11.55 kcal/mol (Table 6), respectively.

This isomerization pathway of AICA was constructed as a series of constrained optimization by taking C=C–C=O torsion angle (ω) at specified values. The

resulting curves were presented in Figure 11. Starting from **A1d** or **A1d'** associated with $\omega \approx 0°$, it is conformational labile and this molecule may initially move along the rotation path at some stage, but finally it will switch to **A1** or **A1'** rotation pathway. Same phenomenon could be observed during rotation of **A2d** and **A3** analogues. Take **A1** as a starting point at torsional angle c.a. 355°, counterclockwise rotating Ar-CO bond will lead to a transition state CC-RTS(**A1,A2'**) at about 280° with higher barrier (11.55 kcal/mol), and a minima structure **A2'** around 210°. Seen from Figure 11(c) clockwise rotation of minima **A3'** at c.a. 190° will result in sharply drop to **A1**'s pathway. Moreover, ITS(**A3,A3'**) at 180° correlate these pathway together and so does ITS(**A2**,**A2d**). As a result of its low barrier, this rotation could contribute to NMR dynamics.

In the several decades, Water dimmer, ammonia dimmer and water-ammonia aggregate have been exhaustively investigated in both experiment and theory. The main focus on these dimmers is their characteristic intermolecular hydrongen bonding, and most HB formation styles are displayed in Scheme 6.

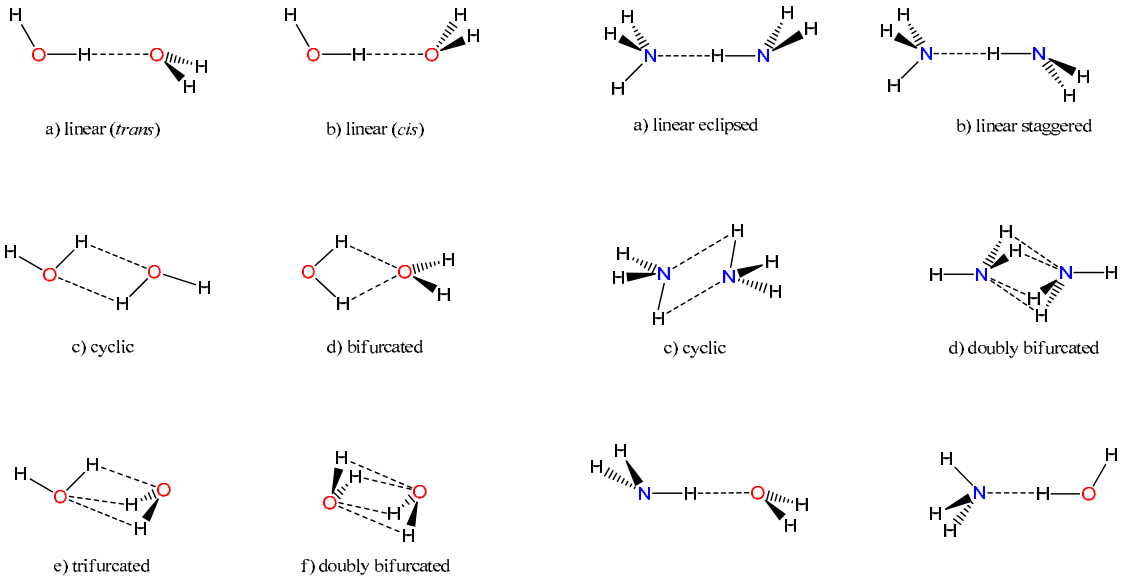

Scheme 6. Structures of dimers of water and ammonia and of the water-ammonia cluster.

For water dimers, [37,38] the linear conformations are more stable than cyclic and multifurcated forms. Ammonia dimmer[39,40] and water-ammonia dimmer[41,42] are

more attractive in that they are analogous to **A2**/**A3** and **A1**, respectively. Like water-ammonia dimmer, Intramolecular H-bonding NH···O=C preferentially stablizes the AICA1 conformation. When rotation of Ar-CO happens, this H-bonds is going to be destroyed, then relatively weak interaction NH···NH will form to generate AICA2 and AICA3, like ammonia-ammonia case. AICA2 features one intramolecular amino-amide H-bond ($NH\cdots NH_2CO$) and four HB-donors are available for interactions with solvent molecules. The H-bond in AICA2 is weaker than the one in AICA1 but it is steady (even in solvents with better HB donors).

4 Conclusion

In our study, we implemented a series of dynamic NMR experiments in two different solvents: acetone, acetonitrile. These dynamic studies indicate AICA compound presents in different conformations. Only one tautomation has been found in both acetone and acetonitrile, while it is well known that there are two tautomers found in natural world. In addition, the distinctive solvent and temperature effects on our sample have been observed during the dynamic experiment. What causes these NMR features is being assumed according to theoretical analysis.

The evaluation of NMR data has been carried out to calculate the barrier of these dynamic processes. The calculated energy barrier is in nice agreement with experiment one as shown in Table 2. On the other end, this indicates two most possible mechanisms to reflect plausible interconversion of AICA and interaction with solvent molecule in aqueous phase.

The future work is directed toward dynamics of AICA in a less polar solvent.

5 Reference

1 (a) A facile synthesis of [N1,NH_2-$^{15}N_2$]-, [N3,NH_2-$^{15}N_2$]-, and [N1,N3,NH_2-$^{15}N_3$]-labeled adenine. Jain, M. L.; Tsao, Y.; Ho, N.; Cheng, J. *J. Org. Chem.* **2001**, *66*, 6472-6475. (b) Nitrogen-15-labeled Deoxynucleosides. 3. Synthesis of [3-15N]-2'- Deoxyadenosine. Rhee, Y. S.; Jones, R. A. *J. Am. Chem. Soc*. **1990**, *112*, 8174-8175.

2 Prebiotic synthesis of nucleotides. Zubay, G.; Mui, T. *Orig. Life Evol. Bios.* **2001**, *31*, 87-102.

3 Heterocyclic compounds recovered from carbonaceous chondrites. Folsome, C. E.; Lawless, J. G.; Romiez, M.; Ponnamperuma, C. *Geochim. Cosmochim. Acta* 1**973**, *37*, 455-65.

4 Orgueil meteorite: organic nitrogen contents. Hayatsu, R. *Science* **1964**, *146*, 1291-1293.

5 Organic compounds in the Murchison meteorite. Ponnamperuma, C. *Ann. NY. Acad. Sci.* **1972**, *194*, 56-69.

6 Heterocyclic compounds indigenous to the Murchison meteorite. Folsome, C. E.; Lawless, J.; Romiez, M.; Ponnamperuma, C. *Nature* **1971**, *232*, 108-109.

7 Purines and triazines in the Murchison meteorite. Hayatsu, R.; Studier, M. H.; Moore, L. P.; Anders, E. *Geochim. Cosmochim. Acta* **1975**, *39*, 471–488.

8 Nitrogen-heterocyclic compounds in meteorites: significance and mechanisms of formation. Stoks, P. G.; Schwartz, A. W. *Geochim. Cosmochim. Acta* **1981**, *45*, 563-569.

9 Survivability of biomolecules during extraterrestrial delivery: new results on pyrolysis of amino acids and poly-amino acids. Basiuk, V. A.; Douda, J. *Adv. Space Res.* **2001**, *27*, 231-236.

10 Extraterrestrial nucleobases in the Murchison meteorite. Martins, Z.; Botta, O.; Fogel, M. L.; Sephton, M. A.; Glavin, D. P.; Watson, J. S.; Dworkin, J. P.; Schwartz, A. W.; Ehrenfreund, P. *Earth Planet. Sci. Lett.* **2008**, *270*, 130-136.

11 (a) Sandström, J. *Dynamic NMR Spectroscopy*. Academic Press: London, **1982**. (b) Barriers to rotation about the chiral axis of tertiary aromatic amides. Ahmed, A.; Bragg, R. A.; Clayden, J.; Lai, L. W.; McCarthy, C.; Pink, J. H.; Westlund, N.; Yasin, S. A. *Tetrahedron* **1998**, *54*, 13277-13294.

12 Frisch, M.J., Trucks, G.W., Schlegel, H.B., Scuseria, G.E., Robb, M.A., Cheeseman, J.R., Montgomery, Jr., J.A., Vreven, T., Kudin, K.N., Burant, J.C., Millam, J.M., Iyengar, S.S., Tomasi, J., Barone, V., Mennucci, B., Cossi, M., Scalmani, G., Rega, N., Petersson, G.A., Nakatsuji, H., Hada, M., Ehara, M., Toyota, K., Fukuda, R., Hasegawa, J., Ishida, M., Nakajima, T., Honda, Y.,

Kitao, O., Nakai, H., Klene, M., Li, X., Knox, J.E., Hratchian, H.P., Cross, J.B., Bakken, V., Adamo, C., Jaramillo, J., Gomperts, R., Stratmann, R.E., Yazyev, O., Austin, A.J., Cammi, R., Pomelli, C., Ochterski, J.W., Ayala, P.Y., Morokuma, K., Voth, G.A., Salvador, P., Dannenberg, J.J., Zakrzewski, V.G., Dapprich, S., Daniels, A.D., Strain, M.C., Farkas, O., Malick, D.K., Rabuck, A.D., Raghavachari, K., Foresman, J.B., Ortiz, J.V., Cui, Q., Baboul, A.G., Clifford, S., Cioslowski, J., Stefanov, B.B., Liu, G., Liashenko, A., Piskorz, P., Komaromi, I., Martin, R.L., Fox, D.J., Keith, T., Al-Laham, M.A., Peng, C.Y., Nanayakkara, A., Challacombe, M., Gill, P.M.W., Johnson, B., Chen, W., Wong, M.W., Gonzalez, C., and Pople, J.A. (2004) Gaussian 03, Revision D.01. Gaussian, Inc., Wallingford, CT.

13 (a) Cramer, C. J. *Essentials of Computational Chemistry, Theories and Models*; John Wiley & Sons: Chichester, UK, **2002**. (b) Hehre, W. J.; Radom, L.; Schleyer, P. R.; Pople, J. *Ab Initio Molecular Orbital Theory*; John Wiley & Sons: New York, **1986**.

14 Note on an Approximation Treatment for Many-Electron Systems. Møller, C.; Pleset, M. S. *Phys. Rev.* **1934**, *46*, 618-622.

15 A comparison of geometry optimization with mixed cartesian and internal coordinates. H. B. Schlegel, *Int. J. Quant. Chem.: Quant. Chem. Symp.* **1992**, *26*, 243-252.

16 (a) Electrostatic interaction of a solute with a continuum. A direct utilization of *ab initio* molecular potentials for the prevision of solvent effects. Miertus, S.; Scrocco, E.; Tomasi, J. *Chem. Phys.* **1981**, *55*, 117-129. (b) Approximate evaluations of the electrostatic free energy and internal energy changes in solution processes Miertus, S.; Tomasi, J. *Chem. Phys.*, **1982**, *65*, 239-245.

17 New universal solvation model and comparison of the accuracy of the SM5.42R, SM5.43R, C-PCM, D-PCM, and IEF-PCM continuum solvation models for aqueous and organic solvation free energies and for vapor pressures. Thompson, J. D.; Cramer, C. J.; Truhlar, D. G. *J. Phys. Chem. A* **2004**, *108*, 6532-6542.

18 (a) Lide, D. R. *Handbook of Chemistry and Physics*, CRC Press, Florida, **2004**. (b). Dielectric and structural results for liquid acetonitrile, acetone and chloroform from the hypernetted chain molecular integral equation. Fries, P. H.; Richardi, J.; Krienke, H. *Molec. Phys.* **1997**, *90*, 841-853.

19 Conformation-directing effects of a single intramolecular amide-amide hydrogen bond: variable-temperature NMR and IR studies on a homologous diamide series. Gellman, S. H.; Dado, G. P.; Liang, G. B.; Adams, B. R. *J. Am. Chem. Soc.* **1991**, *113*, 1164-1173.

20 Tautomeric and conformational properties of malonamide, $H_2C(O)$-CH_2-$C(O)NH_2$: Electron diffraction and quantum chemical study. Belova, N. V.;

Oberhammer, H.; Girichev, G. V.; Shlykov, S. A. *J. Phys. Chem. A* **2007**, *111*, 2248 -2252.

21 Molecular mechanics calculations of conjugated amides and an *ab initio* investigation of acrylamide and its β-amino derivative: Conformational analysis and rotational barriers. Berg, U.; Bladh, N. *J. Comput. Chem.* **1996**, *17*, 396-408.

22 Evidence for intramolecular N-H···O resonance-assisted hydrogen bonding in β-enaminones and related heterodienes. A combined crystal-structural, IR and NMR spectroscopic, and quantum-mechanical investigation. Gilli, P.; Bertolasi, V.; Ferretti, V.; Gilli, G. *J. Am. Chem. Soc.* **2000**, *122*, 10405-10417.

23 Intramolecular hydrogen bonding in ortho-substituted *N*,*N*-dimethyl benzamides. Fong, C. W. *Aust. J. Chem.* **1980**, *33*, 1285-1290.

24 Precursors in the biosynthesis of purine nucleotides. The crystal structures of 5-amino-1-β-D-ribofuranosylimidazole-4-carboxamide (AICAR) and its 5'-(dihydrogenphosphate). Adamiak, D. A.; Saenger, W. *Acta Cryst.* **1979**, *B35*, 924-928.

25 Structure of 5-amino-1-diphenylmethylimidazole-4-carboxamide. Banerjee, T.; Roychowdhury, P.; Chattopadhyay, D.; Ray, S.; Chatterjee, G.; Kashino, S.; Haisa, M. *Acta Cryst.* **1991**, *C47*, 804-847.

26 5-amino-1-[2-(diethylamino)ethyl]-1*H*-imidazole-4-carboxamide. Dey, R.; Banerjee, T.; Langer, V.; Ray, S.; Roychowdhury, P. *Acta Cryst.* **2006**, *E62*, 814-816.

27 Synthesis and crystal structures of 5-amino-1-(2-hydroxyethyl)imidazole-4-carboxamide and 5-amino-1-(2-chloroethyl)-4-cyanoimidazole. Banerjee, T.; Chaudhuri, S.; Moore, M.; Ray, S.; Chatterjee, P. S.; Roychowdhury, P. *J. Chem. Crystollogr.* **1999**, *29*, 1281-1286.

28 Synthesis and crystal structure of (5-amino-4-carboxamido imidazol -1-yl)acetamide, a possible PDE inhibitor. Banerjee, T.; Roychowdhury, P.; Yamane, T.; Ray, S.; Pathak, K. *J. Cryst. Spectrosc. Res.* **1991**, *2*1, 121-125.

29 Structures of three forms of the purine base precursor 5(4)-amino-1H -imidazole-4(5)-carboxamide (AICA): AICA.C_3H_7OH, AICA.H_2O and $HAICA^+$.H2PO4$^-$. Simon, K.; Schawartz, J.; Kalman, A. *Acta Cryst.* **1980**, *B36*, 2323-2328.

30 Structure of acetone and dimethyl sulfoxide from Monte Carlo simulations and MM2 calculations. Cordeiro, J. M. M. *Phys. Chem. Liquids* **2007**, *45*, 31-39.

31 (a) Monte Carlo simulations of the solution structure of simple alcohols in water-acetonitrile mixtures. Nagy, P. I.; Erhardt, P. W. *J. Phys. Chem. B*

2005, *109*, 5855-5872. (b) Structural information about formamide and *N*-methylformamide in the pure liquid and in mixture with acetonitrile-d3 (CD_3CN). A nuclear magnetic relaxation study. Leiter, H.; Mal, S.; Hertz, H. G. *Z. Phys. Chem.* **1983**, *136*, 101-115. (c) Pictorial intuition of the correlation between structure and properties in liquid solutions: acetonitrile as a strongly structured solvent of dissociated ions. Fries, P. H.; Kunz, W.; Calmettes, P.; Turq, P. *Theochem* **1995**, *330*, 287-300.

32 Evaluation of the catalytic mechanism of AICAR Transformylase by pH-dependent kinetics, mutagenesis, and quantum chemical calculations. Shim, J. H.; Wall, M.; Benkovic, S. J.; Diaz, N.; Suarez, D.; Merz, K. M. Jr *J. Am. Chem. Soc.* **2001**, *123*, 4687-4696.

33 (a) Theoretical study of one-carbon unit transfer between methyl-AICA and N^1-methyl-N^1-acryloyl-formamide. Qiao, Q.; Cai, Zh.; Feng, D.; Jiang, Y. . *Int. J. Quant. Chem*. **2005**, *101*, 33-39. (b) The catalytic mechanism of one-carbon unit transfer between AICA and N10-formyl-tetrahydrofolate: An ONIOM study. Qiao, Q.; Cai, Zh.; Feng, D.; Jiang, Y. *J. Mol. Struct*. (Theochem) **2005**, *713*, 7-13.

34 Non-biaryl atropisomers: New classes of chiral reagents, auxiliaries, and ligands. Clayden, J. *Angew. Chem., Int. Ed. Engl.* **1997**, *36*, 949-951.

35 Stereodynamics of bond rotation in tertiary aromatic amides. Bragg, R. A.; Clayden, J.; Morris, G. A.; Pink, J. H. *Chem. Eur. J.* **2002**, *8*, 1279-1289.

36 (a) Exchange of amide protons. Effect of intermolecular hydrogen bonding. Perrin, C. L.; Dwyer, T. J.; Rebek, J.; Duff, R. J. *J. Am. Chem. Soc.* **1990**, *112*, 3122-3125. (b) Conformation-directing effects of a single intramolecular amide-amide hydrogen bond: Variable-temperature NMR and IR studies on a homologous diamide series. Gellman, S. H.; Dado, G. P.; Liang; Adams, B. R. *J. Am. Chem. Soc.* **1991**, *113*, 11264-11173.

37 Spectroscopic determination of the water dimer intermolecular potential-energy surface. Goldman, N.; Fellers, R. S.; Brown, M. G.; Braly, L. B.; Keoshian, C. J.; Leforestier, C.; Saykally, R. J. *J. Chem. Phys*. **2002**, *116,* 10148-10163.

38 (a) Ab initio non-orthogonal approaches to the computation of weak interactions and of localized molecular orbitals for QM/MM procedures. Raimondi, M.; Famulari, A.; Specchio, R.; Sironi, M.; Moroni, F.; Gianinetti, E. *J. Mol. Struct. (Theochem)* **2001**, *573*, 25-42. (b) Characterizing the potential energy surface of the water dimer with DFT: Failures of some popular functionals for hydrogen bonding. Anderson, J. A.; Tschumper, G. S. *J. Phys. Chem. A* **2006**, *110*, 7268-7271. (c) Anchoring the water dimer potential energy surface with explicitly correlated computations and focal point analyses. Tschumper, G. S.; Leininger, M. L.; Hoffman, B. C.; Valeev,

E. F.; Schaefer, H. F., III; Quack, M. *J. Chem. Phys.* **2002**, *116*, 690-701. (d) Ab initio studies of hydrogen bonds: the water dimer paradigm. Scheiner S. *Annu. Rev. Phys. Chem.* **1994**, *45*, 23-56.

39 Tunneling motions and spectra of hydrogen bonded complexes; the ammonia dimer and the water trimer. Van Der Avoird, A. D.; Wormer, P. E. S. *NATO ASI Series, Series C: Mathematical and Physical Sciences* **2000**, *561*, 29-153.

40 (a) Ab initio and DFT calculations of some weakly bound dimers and complexes. I. The dimers of ammonia and phosphine. Altmann, J. A.; Govender, M. G.; Ford, T. A. *Mol. Phys.* **2005**, *103*, 949-961. (b) The spin-spin coupling constants in the ammonia dimer. Pecul, M.; Sadlej, J. *Chem. Phys. Lett.* **2002**, *360*, 272-282.

41 Raman spectral analysis of liquid ammonia and aqueous solution of ammonia. Ujike, T.; Tominaga, Y. *J. Raman Spectr.* **2002**, *33*, 485-493.

42 (a) Comparison of two ways to decompose intermolecular interactions for hydrogen-bonded dimer systems. Langlet, J.; Caillet, J.; Berges, J.; Reinhardt, P. *J. Chem. Phys.* **2003**, *118*, 6157-6166. (b) H-bond vibrations in ammonia-ammonia and ammonia-water dimers. Bende, A.; Suhai, S. *Acta Physica et Chimica Debrecina* **2005**, 55-67.

Appendix 1: Linear Regression Curves.

Figure A1. Linear regression curves for AICA in D_3-Acetone.

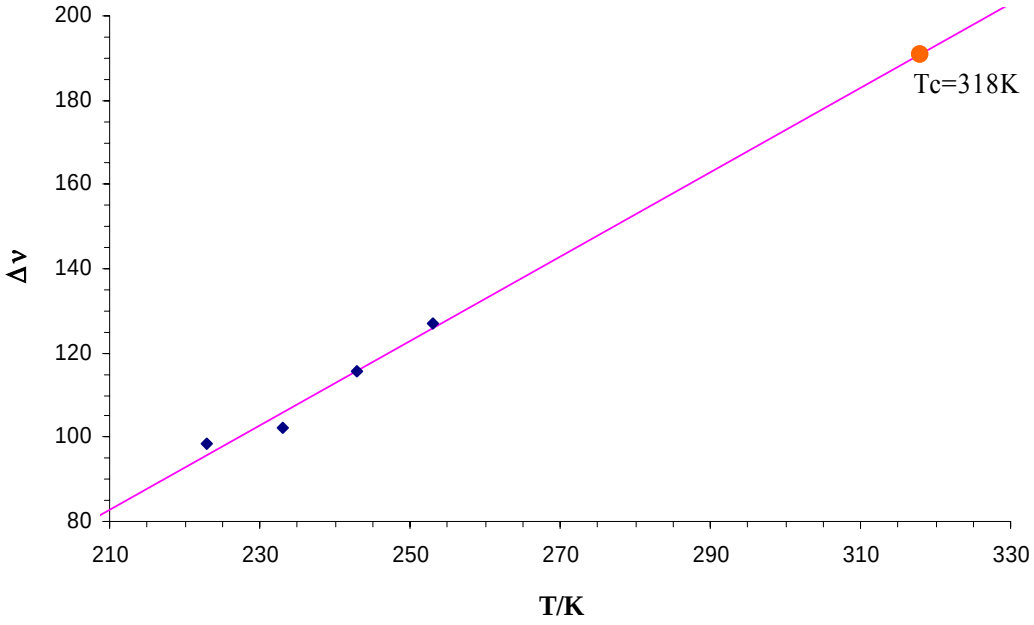

Figure A2. Linear regression curves for AICA in D_3-Acetonitrile.

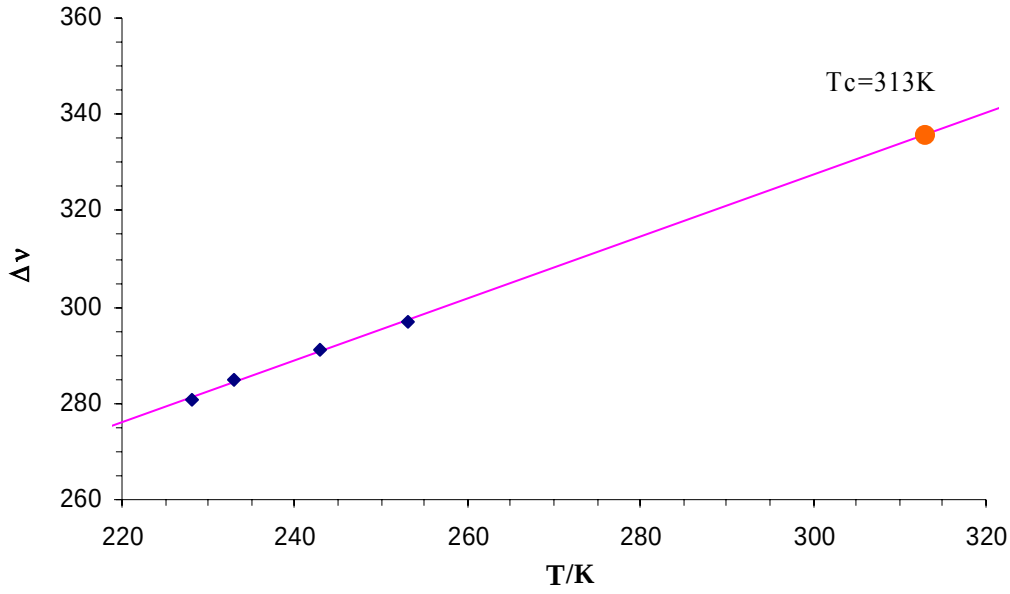

Appendix 2: MP2(full)/6-311++G** Data

Table A1. Total Energies and Thermodynamical Data for AICA in Gas Phase[a,b]

Geometry		*E*	*VZPE*	*TE*	*S*	*NIF*	*lowest* ν_1	μ
AICA1 := **A1**	C_1	-449.393642	72.24	77.47	88.65	0	78	4.75
AICA1-dia := **A1d**	C_1	-449.393470	72.21	77.45	88.56	0	74	4.87
AICA2 := **A2**	C_1	-449.377695	72.24	77.44	89.06	0	59	7.27
AICA2-dia := **A2d**	C_1	-449.376576	72.14	77.41	89.62	0	62	7.59
AICA3 := **A3**	C_1	-449.376702	72.03	77.29	89.93	0	41	9.55
RTS1(**A1**,**A1d'**)	C_1	-449.363658	71.40	76.36	87.32	1	**i**451	4.60
RTS2(**A1**,**A1d'**)	C_1	-449.366075	71.43	76.41	87.43	1	**i**420	6.83
ITS(**A1**,**A1d'**)	C_1	-449.393189	71.55	76.63	88.04	1	**i**439	4.57
ITS(**A1**,**A1d**)	C_1	-449.388860	70.85	76.19	89.91	1	**i**755	5.18
RTS(**A1**,**A1d**)	C_1	-449.390123	71.94	76.89	87.74	1	**i**241	3.74
RTS2(**A1**,**A1d**)	C_1	-449.378533	71.43	76.47	88.52	1	**I**249	6.31
RTS(**A2**,**A2d'**)	C_1	-449.365638	71.57	76.42	86.19	1	**i**283	6.93
ITS(**A2**, **A2d**)	C_1	-449.372307	71.14	76.41	91.21	1	**i**594	8.73
RTS(**A2**,**A2d**)	C_1	-449.375292	71.95	76.87	88.10	1	**i**162	6.44
MPTSR-TS	C_1	-449.348304	70.97	76.16	90.50	1	**i**380	8.19
ITS(**A3**,**A3'**)	C_s	-449.376088	71.17	76.33	90.55	1	**i**378	9.61
RTS(**A3**,**A3'**)	C_1	-449.347992	70.95	76.14	90.60	1	**i**400	10.24
RTS(**A2**,**A3'**)	C_1	-449.375612	71.73	76.63	86.59	1	**i**168	9.13
RTS(**A2d**,**A3'**)	C_1	-449.369388	71.43	76.52	89.87	1	**i**213	8.54
CC-RTS(**A1**,**A2'**)	C_1	-449.374739	71.96	76.90	87.81	1	**i**77	5.36
CC-RTS(**A1**,**A3'**)	C_1	-449.369795	71.40	76.50	87.81	1	**i**80	7.69

[a] All data computed at MP2(full)/6-311++G**.

[b] Total energies *E* in hartrees, vibrational zero-point energies *VZPE* and thermal energies *TE* in kcal/mol, entropies *S* in cal/mol K, number of imaginary frequencies *NIF*, values of the lowest vibrational frequency ν_1 (imaginary or real), and electric dipole moments μ in Debye (D).

Table A2. Total Energies and Thermodynamical Data for AICA Considering Bulk Solvent.[a,b]

Geometry		E_{SP}	E	*VZPE*	*TE*	S	*NIF*	*lowest* ν_1	μ
In Acetone									
AICA1 := **A1**	C_1	-449.422519	-449.423987	70.40	75.76	91.29	0	28	6.87
AICA1-dia := **A1d**	C_1	-449.422544	-449.423997	70.57	75.81	88.53	0	88	7.21
AICA2 := **A2**	C_1	-449.414268	-449.416722	70.64	75.88	89.27	0	67	12.09
AICA2-dia := **A2d**	C_1	-449.412987	-449.415046	70.67	75.91	89.01	0	88	11.93
RTS1(**A1**,**A1d'**)	C_1	-449.396663	-449.398049	69.91	74.81	86.37	1	**i**427	7.30
RTS2(**A1**,**A1d'**)	C_1	-449.398276	-449.399783	69.92	74.86	86.77	1	**i**381	10.00
CC-RTS(**A1**,**A2'**)	C_1	-449.408386	-449.410270	70.02	75.10	88.81	1	**i**70	9.56
RTS(**A2**,**A2d'**)	C_1	-449.399364	-449.400778	70.15	74.94	85.62	1	**i**343	10.73
In Acetonitrile									
AICA1 := **A1**	C_1	-449.423711	-449.425401	70.43	75.69	88.66	0	89	6.99
AICA1-dia := **A1d**	C_1	-449.423770	-449.425405	70.48	75.72	88.53	0	88	7.36
AICA2 := **A2**	C_1	-449.415899	-449.418623	70.53	75.78	89.42	0	62	12.36
AICA2-dia := **A2d**	C_1	-449.414640	-449.416972	70.56	75.81	89.12	0	90	12.21
RTS1(**A1**,**A1d'**)	C_1	-449.398136	-449.399678	69.82	74.72	86.37	1	**i**425	7.44
RTS2(**A1**,**A1d'**)	C_1	-449.399668	-449.401348	69.83	74.76	86.76	1	**i**380	10.16
CC-RTS(**A1**,**A2'**)	C_1	-449.409868	-449.412020	69.90	74.98	88.58	1	**i**69	9.88
RTS(**A2**,**A2d'**)	C_1	-449.400829	-449.402412	70.06	74.86	85.60	1	**i**346	10.92

[a] All data computed at PCM(MP2(full)/6-311++G**). Energies E_{SP} are based on the MP2(full)/6-311++G** optimized structures. All other data are based on the PCM-optimized structures.

[b] Total energies E in hartrees, vibrational zero-point energies *VZPE* and thermal energies *TE* in kcal/mol, entropies S in cal/mol K, number of imaginary frequencies *NIF*, values of the lowest vibrational frequency ν_1 (imaginary or real), and electric dipole moments μ in Debye (D).

Appendix 3: Gas Phase Cartesian Coordinates of (MP2(full)/6-311 ++G**) Optimized Minima Structures

AICA Related Stuffs in Gas Phase

A1
0,1
C,-0.0050102984,0.1493396285,0.1313544396
C,-0.014597789,-0.0810225315,2.2633875464
C,1.3219236596,-0.0816566162,1.8944262825
N,1.3082543227,0.0633136297,0.5305700317
H,2.1174466341,0.0150260028,-0.0722134932
H,-0.2851914356,0.2855264552,-0.9031740072
N,-0.8299648144,0.0658693712,1.1572374719
N,2.4810656198,-0.302175969,2.6267131958
H,3.1802131464,0.4216947556,2.5062383847
H,2.232076128,-0.3988477344,3.6086291266
C,-0.5034159092,-0.1914457656,3.6422875356
O,0.2622972542,-0.4079502537,4.5849571655
N,-1.8443981684,0.0108079488,3.7877700142
H,-2.4159965741,-0.0092860124,2.9557650339
H,-2.2546496619,-0.2510298354,4.6707400248

A1d
0,1
C,-0.0073572168,0.0158575975,-0.0068043686
C,0.0024381919,0.0299481094,2.13794384
C,1.3317865739,-0.0807653564,1.7595742403
N,1.3071112271,-0.0800256039,0.3882841767
H,2.1179564715,-0.0565518556,-0.2137630741
H,-0.2974490405,0.0150122471,-1.0475476212
N,-0.8211058879,0.0811902911,1.0288147055
N,2.5038505687,-0.067664477,2.5034039589
H,3.1370876385,-0.8251193695,2.2742884007
H,2.2611456006,-0.0924577295,3.4913917391
C,-0.4772604385,0.030548463,3.5244698064
O,0.2998337641,-0.0603368437,4.4785043462
N,-1.8255335391,0.1802980198,3.6598384959
H,-2.400167501,0.0615845149,2.8385728753
H,-2.2211165664,0.0001676078,4.5694069607

A2
0,1
C,0.0201343127,-0.074341131,0.1632170927
C,0.0027497912,0.1122314569,2.2984628964
C,1.3427949206,0.0053184516,1.938448192
N,1.3329992887,-0.118873611,0.5736886536

H,2.1427452685,-0.2785128801,-0.0088574189
H,-0.2586250309,-0.1498092297,-0.8780751382
N,-0.804587512,0.0711636834,1.1779935404
N,2.5344883634,-0.0432350762,2.6678807237
H,3.2352866304,0.5952554717,2.3071297071
H,2.3550336285,0.1733112499,3.6434166436
C,-0.530952342,0.3226537055,3.6566595618
O,-1.5219829062,0.980784088,3.9148342522
N,0.275075984,-0.2498795203,4.6523084249
H,-0.149877045,-0.1974699165,5.570524409
H,0.6307024915,-1.1717918402,4.4310849526

A2d
0,1
C,-0.0135530286,0.0108506192,-0.0057656822
C,0.0168349159,-0.0251956458,2.137127786
C,1.34960315,-0.0731740472,1.7375476918
N,1.3060496587,-0.0521966145,0.3667389359
H,2.1129915878,0.0455021493,-0.233620621
H,-0.321475454,0.0060057181,-1.0416913543
N,-0.816407086,0.038029839,1.0388366159
N,2.575930286,-0.0034032023,2.4130005765
H,3.1258022025,-0.8515828515,2.328782464
H,2.4267341688,0.2035410121,3.3944736764
C,-0.51061243,0.0491109656,3.5168887282
O,-1.5237918394,0.6490367066,3.8246151423
N,0.310918577,-0.5712744657,4.4652645685
H,-0.1255759121,-0.6290382964,5.3773067759
H,0.7332553142,-1.4394479856,4.1640146687

A3
0,1
C,0.0487974662,0.1245603951,0.1625912544
C,-0.0297435642,0.0298300273,2.3040139585
C,1.3192564132,-0.0242177668,1.9691312097
N,1.3442141089,0.0339181025,0.5905295945
H,2.1728982822,0.0174223081,0.0121732984
H,-0.2116055164,0.1840108792,-0.8850264648
N,-0.8031737413,0.1264102815,1.170721636
N,2.4643049381,-0.1239341993,2.7896917405
H,3.0983179399,0.6594260483,2.6753367586
H,2.9691586918,-0.9938776256,2.6564471034
C,-0.6582054842,0.0334041374,3.6571221758
O,-1.8427450004,0.2720652294,3.8251971892
N,0.1969654967,-0.3060374193,4.6798571691
H,1.1921822212,-0.2295795117,4.5129348985
H,-0.1492026042,-0.1166365486,5.6089207669

AICA Transition States in Gas Phase
RTS1(**A1**,**A1d'**)

0,1
C,0.0166617877,0.0344973565,-0.0213167642
C,-0.0439744746,-0.0027008216,2.1199666173
C,1.3106438328,-0.006182369,1.7752353793
N,1.3302482709,0.0159434385,0.409801867
H,2.1530271195,-0.0637504941,-0.1709766191
H,-0.2367058233,0.0680226297,-1.0714660096
N,-0.8321437199,0.0285315048,0.9801622253
N,2.445414755,-0.125381841,2.5524027699
H,3.2093286362,0.4830266541,2.2865503251
H,2.2030828041,-0.0358129803,3.5351366292
C,-0.512900431,0.0197767967,3.4942575771
O,0.2800847145,-0.0250787252,4.4341041676
N,-1.9384191967,0.1004043305,3.6727537601
H,-2.2086192853,-0.6955069102,4.247983216
H,-2.1158311671,0.9182513381,4.2532753605

RTS2**(A1**,**A1d')**

0,1
C,0.0101548388,0.0382230328,-0.0089392298
C,-0.0130737531,0.0339216208,2.1368834502
C,1.3309681924,-0.0019656824,1.7714546919
N,1.325685706,-0.0018355246,0.4034120155
H,2.1368537353,-0.105157992,-0.1901865303
H,-0.2616804679,0.0630233212,-1.054446019
N,-0.8202730892,0.0637462267,1.0116492096
N,2.4767099645,-0.1363199024,2.532625249
H,3.2330934638,0.4832335529,2.2697051604
H,2.2451441787,-0.0525183296,3.5186384718
C,-0.5010695332,0.0822492934,3.5140512188
O,0.2780326982,0.0316614151,4.4555048931
N,-1.9187491295,0.1933454778,3.7236850347
H,-2.2377057102,1.0181305134,3.2169642864
H,-2.3585115213,-0.5793503775,3.2249279909

ITS**(A1**,**A1d')**

0,1
C,-0.0110778728,-0.0064719636,0.1205649459
C,0.0050329918,-0.0408207901,2.2650778759
C,1.3368067701,0.0039900828,1.8828506266
N,1.3075507833,0.0176074811,0.5114121145
H,2.1142580972,-0.045560549,-0.093326869
H,-0.3044424318,0.0175359791,-0.9189908546
N,-0.8237920615,-0.0385770555,1.1589056844

N,2.510158374,-0.0800872318,2.6209097247
H,3.1728140451,0.6576945754,2.4111528687
H,2.2706203742,-0.0729044715,3.6101002054
C,-0.4684675878,-0.0210407396,3.6545053113
O,0.3171849113,-0.040383828,4.6065856965
N,-1.8191774806,0.0176802784,3.7896563196
H,-2.4034452542,0.0529564914,2.9690254257
H,-2.2169709976,0.0439516932,4.7139933249

ITS**(A1**,**A1d)**

0,1
C,-0.0180033364,0.0078872179,-0.0216851949
C,-0.0108725176,0.0202804682,2.1241179722
C,1.3248898408,-0.0502056615,1.747462986
N,1.3042521837,-0.0512534885,0.3766392433
H,2.1062863378,-0.1020738279,-0.2342824758
H,-0.3007704184,0.0182733111,-1.0642412242
N,-0.8321855591,0.0509201892,1.0109011992
N,2.4476929328,-0.1057551817,2.5150758112
H,3.3719386022,-0.1297642577,2.1262136202
H,2.2984621966,-0.1277969684,3.5135798235
C,-0.4736188939,0.0305727767,3.5086865052
O,0.3165224242,-0.0687814626,4.4535492612
N,-1.8194273923,0.2066945072,3.668294705
H,-2.4065500442,0.0710006902,2.858237858
H,-2.1981346998,0.0032192457,4.5803615764

RTS1**(A1**,**A1d)**

0,1
C,-0.006297196,0.0045395416,0.0184902184
C,0.0045571916,-0.0008783804,2.1644077884
C,1.3376937504,-0.0559474373,1.7814453128
N,1.2993029257,-0.0485006113,0.4089114687
H,2.1232928571,-0.071185709,-0.1767623029
H,-0.3073198495,0.016962643,-1.0191647148
N,-0.8214788337,0.0355544834,1.063105383
N,2.574687883,-0.1027288972,2.4558076322
H,2.6260591197,0.6689628932,3.1142017681
H,2.6195112351,-0.9466175014,3.0196120836
C,-0.50558638,0.0032519534,3.5510892156
O,0.2372570866,-0.1290660629,4.5210624136
N,-1.8510378624,0.2118266166,3.6430089058
H,-2.4020251217,0.1180409299,2.8021121057
H,-2.282916475,0.0359101278,4.5369555225

RTS2**(A1**,**A1d)**
0,1

C,-1.5896209801,-1.5165202134,-0.0553108231
C,0.1184699369,-0.2079099944,-0.0194028532
C,-0.9910077721,0.6268123016,0.0239821054
N,-2.0694751791,-0.2424703148,0.0000374991
H,-3.0403619684,0.0365983736,0.0331326263
H,-2.2331335886,-2.3841081867,-0.0947321276
N,-0.2667774931,-1.5311052048,-0.0645526175
N,-1.0999107015,2.0178624388,0.0951339631
H,-1.5958502712,2.4460833613,-0.6737436634
H,-1.395862106,2.3767527599,0.9921442386
C,1.5598614946,0.1616733078,-0.0279239238
O,1.9661810864,1.3031298448,-0.1907052001
N,2.3800051242,-0.9116951395,0.2116312072
H,1.985487667,-1.8347276934,0.101351226
H,3.3582605783,-0.7767483748,0.0062706465

ITS**(A2,A2d)**

0,1
C,1.8977705535,-1.2332619308,0.1077237801
C,-0.0625490837,-0.3627804846,0.0413819167
C,0.8301873147,0.702792001,-0.0541860697
N,2.0755172956,0.1303021138,-0.0005875594
H,2.952030588,0.6098912277,-0.1474759591
H,2.7327029765,-1.9132933121,0.1985111862
N,0.6254793118,-1.5593709866,0.1250823146
N,0.6454613944,2.0556640251,-0.2215958504
H,1.3588144595,2.7201932204,0.0163772642
H,-0.2287752056,2.3844305917,-0.5941265942
C,-1.5341794169,-0.310145658,-0.0163901932
O,-2.2383547223,-1.2406050167,-0.3646159064
N,-2.0640391894,0.94973052,0.2990377841
H,-3.0702920037,0.9201099461,0.4089498182
H,-1.5921941741,1.4344679824,1.0520800215

RTS**(A2,A2d)**
0,1
C,0.0000077585,0.0005817832,-0.000112199
C,-0.0001874103,-0.0002091504,2.1427633949
C,1.3398785842,-0.0003667077,1.7638751115
N,1.306438327,0.0026208648,0.3899120614
H,2.1319567595,0.0396337531,-0.1925471498
H,-0.3000965214,-0.0139732536,-1.0381879474
N,-0.8204644855,0.0050925252,1.0395166192
N,2.5860665738,0.0768417057,2.4242084004
H,2.7494200489,-0.7290280177,3.0157033758
H,2.6354947166,0.9041207097,3.0089655189
C,-0.5548831346,0.0595400919,3.5195762279
O,-1.4627759117,0.8038631671,3.8453635559

N,0.1078040846,-0.7604633931,4.42264519
H,-0.3451781439,-0.8333380831,5.3245855425
H,0.4697943791,-1.6291290352,4.0572072456

RTS**(A2,A2d')**
0,1
C,-0.0027497812,0.1767446764,-0.0096937918
C,-0.0064402192,-0.0510191435,2.1231053876
C,1.3397138193,-0.0548150357,1.7410422552
N,1.3180823666,0.0931123104,0.3811714799
H,2.1234930531,0.0327297788,-0.2257515246
H,-0.2843324178,0.3143306392,-1.0442310802
N,-0.8222330987,0.0954611495,1.0106956482
N,2.5196696964,-0.2737577704,2.4336869259
H,3.2556498309,0.3824448242,2.2013528913
H,2.3145532125,-0.2769329703,3.4314189921
C,-0.5481399189,-0.166124201,3.4689389297
O,-1.7303175058,-0.179478323,3.7443998442
N,0.4964847073,-0.2670640003,4.4984377758
H,0.3256599185,0.5058138379,5.141745327
H,0.2705845536,-1.0988848589,5.0435416443

ITS**(A3,A3')**
0,1
C,-0.0006224894,0.,-0.0025651929
C,0.0016588258,0.,2.1428872209
C,1.3388263849,0.,1.7593272196
N,1.3120897276,0.,0.3794719069
H,2.1194714005,0.,-0.2284751171
H,-0.300832625,0.,-1.0411915149
N,-0.8149734721,0.,1.0361479786
N,2.5165653141,0.,2.5394259536
H,3.083082786,0.8290721487,2.3948204546
H,3.083082786,-0.8290721487,2.3948204546
C,-0.5830875991,0.,3.517149085
O,-1.7881300817,0.,3.7129369804
N,0.3443676709,0.,4.5224598924
H,1.3332785078,0.,4.3177208645
H,0.0054200146,0.,5.4708443246

RTS**(A3,A3')**

0,1
C,1.8602389124,-1.2635592679,0.1262294254
C,-0.0819115283,-0.3561929322,0.0343268446
C,0.8313564466,0.6923300829,-0.053019683
N,2.0679438277,0.0830114007,0.0069111776
H,2.9605461371,0.5547114354,-0.0437590274
H,2.6748115025,-1.9700446989,0.2062195845

N,0.5752875834,-1.5628074612,0.1396531904
N,0.6318550616,2.0766582232,-0.2275285254
H,1.0597186207,2.4311533139,-1.0753153159
H,0.9340896858,2.6281309914,0.5677101554
C,-1.5667672227,-0.2888390777,-0.0419976737
O,-2.2195237727,-1.2307389229,-0.4294867056
N,-2.1959825311,0.9458822916,0.3647599735
H,-1.8479765216,1.1765852928,1.2938002864
H,-1.8287173293,1.6895565024,-0.2274068289

RTS**(A2d,A3')**

0,1
C,1.8461448381,-1.2681269383,0.2079802208
C,-0.0753698526,-0.3310389894,0.036535513
C,0.8534670459,0.6931988312,-0.1073190447
N,2.0774782718,0.0667122134,0.0099252892
H,2.9792658407,0.519369795,-0.0415739492
H,2.647093283,-1.9850007935,0.3204290437
N,0.5544547839,-1.5394750731,0.2364329092
N,0.6962334894,2.0526548424,-0.4073124756
H,1.4633998869,2.44823214,-0.9336261199
H,0.4590313393,2.6362130474,0.3833342471
C,-1.5545981511,-0.2432297372,-0.0666647592
O,-2.2219695993,-1.0137859622,-0.735420457
N,-2.101143658,0.8266703218,0.6190111969
H,-3.1110097579,0.8263864229,0.6702005549
H,-1.6221527689,1.1315624133,1.4523371681

CC-RTS**(A1,A3')**

0,1
C,-0.001053397,0.0149902104,0.0073944586
C,0.0107337531,-0.006150323,2.1494331033
C,1.3417018291,-0.0083052605,1.774103097
N,1.3103749904,-0.0005384082,0.3906775661
H,2.1148787422,-0.0343326574,-0.219390335
H,-0.3040891009,0.0521696888,-1.0293935306
N,-0.816453811,0.0029408799,1.0514154417
N,2.4958314737,-0.049883127,2.570983897
H,2.8536988776,-0.9853765072,2.720619344
H,3.2312124272,0.573338182,2.2641994674
C,-0.513022659,-0.1048763838,3.5460420822
O,-0.8374409981,-1.1689075183,4.0515425198
N,-0.6232367258,1.098271006,4.1857075762
H,-0.1794758786,1.9123572862,3.7944974323
H,-0.8350213868,1.0885348857,5.1725144384

CC-RTS**(A1,A2')**

0,1
C,1.8839273744,-1.2366497386,0.1031619125
C,-0.0544375944,-0.3334862266,-0.0210713814
C,0.8495650832,0.716380466,-0.0468332808
N,2.0821422166,0.1099604874,0.0319073238
H,2.9607850001,0.6094966437,0.0391968697
H,2.6963202576,-1.9455326545,0.1726328771
N,0.59204396,-1.5419171709,0.0771048724
N,0.74677775,2.1196443005,-0.1396613138
H,0.4648974238,2.409833192,-1.070122579
H,0.0699167389,2.4794833998,0.5235539608
C,-1.5393475094,-0.2247514991,-0.1201103168
O,-2.1573834501,-0.4089482633,-1.1557449794
N,-2.1367340654,0.185604562,1.0528755787
H,-1.6469381659,-0.0101937202,1.9130058646
H,-3.1451700194,0.1118252218,1.0832885916

RTS**(A2,A3')**

0,1
C,0.0000179006,-0.0003991995,0.0000069649
C,-0.0000535849,0.0004015985,2.1458771288
C,1.3374149416,0.0005301031,1.7641071215
N,1.3179698248,0.0010824037,0.390889412
H,2.1232367676,-0.0478126138,-0.2173022538
H,-0.2903552877,0.022385511,-1.0407480735
N,-0.8151432554,-0.0109525426,1.0331439201
N,2.5142001214,0.0344683521,2.5293727936
H,3.3505273644,0.185124824,1.9799475882
H,2.6218335426,-0.7870852095,3.114238716
C,-0.5639541223,0.0126838976,3.5163228985
O,-1.7405170673,-0.1955726402,3.7563703502
N,0.3786624708,0.2222768657,4.51412969
H,1.2029989328,0.7547607536,4.2671830367
H,-0.0284045013,0.4336587396,5.4149296864

MPTSR-TS

0,1
C,-1.854646932,-1.2822762687,-0.0886005246
C,0.0778458226,-0.3476980498,0.008799262
C,-0.85947409,0.6924593456,0.032448085
N,-2.0762573057,0.0628558728,-0.0299854713
H,-2.9602790717,0.553880223,-0.0437878246
H,-2.6579665612,-2.0031108735,-0.1483225623
N,-0.5659596827,-1.5651363965,-0.0664344487

N,-0.8501774029,2.1022005305,0.111908094
H,-0.5779543868,2.4412177461,1.0273621405
H,-0.2601247804,2.5263742347,-0.5919248903
C,1.5583859472,-0.2935596142,0.0737656793
O,2.2250199218,-1.2880200471,0.2425010637
N,2.2009072912,0.9987280093,-0.0797277508
H,1.94218552,1.3996874814,-0.9774176438
H,1.865952123,1.6339235505,0.6389451782

Appendix 4: Solution Cartesian Coordinates of (PCM/MP2(full) /6-311++G**) Optimized Structures for AICA.

AICA Minima and Transition States in Acetone

A1
0,1
C,0.0151883815,0.0132228582,0.008636982
C,-0.0138836574,-0.0148747698,2.1589704778
C,1.3294404146,-0.0121935449,1.7901985019
N,1.3209440576,-0.0063605632,0.4238849439
H,2.1488941554,-0.0149735542,-0.186090762
H,-0.2548044649,0.0334191684,-1.0415173605
N,-0.8214078011,0.0079383015,1.0329213297
N,2.4891682143,-0.1206614993,2.5340065639
H,3.2672826329,0.4276025639,2.1671933901
H,2.3176238844,0.0812935143,3.5152893063
C,-0.5189873839,0.016402258,3.5289244261
O,0.2509793875,-0.0562878977,4.5025397141
N,-1.86090801,0.1789520673,3.6617612354
H,-2.4547247992,0.0422508276,2.8510514406
H,-2.2641107698,0.013575712,4.5800347991

A1d
0,1
C,0.0152572839,-0.0013081959,0.0079515853
C,-0.01391042,0.0210956305,2.1585022728
C,1.3294640755,0.007594162,1.7897487417
N,1.3209981871,0.0091212903,0.4234253059
H,2.1489215322,0.0131873605,-0.1866415
H,-0.2551795637,-0.0166646458,-1.0421468539
N,-0.8214398589,0.0056066084,1.0321556711
N,2.4893085657,0.1057001461,2.5349086478
H,3.2713731133,-0.426374809,2.1528492015
H,2.3201794367,-0.124863199,3.510354293
C,-0.5195370769,-0.0293018286,3.5275087981
O,0.2549501506,-0.0511118004,4.5006719336
N,-1.8702854161,-0.0026486038,3.6632761668
H,-2.4502234823,-0.1835035503,2.8512611537

H,-2.2533759519,-0.2200047588,4.5794019132

A2
0,1
C,0.0067458227,0.0535782212,0.0124602882
C,-0.018468092,0.0013838358,2.1636152804
C,1.3257796655,-0.0139575882,1.7872338912
N,1.3127912376,0.0089112512,0.4217387135
H,2.1399250091,0.0242532931,-0.1900764587
H,-0.2677380886,0.0755492123,-1.0364994287
N,-0.8252951461,0.0590686699,1.0391470206
N,2.5058381238,-0.1129832549,2.5146834798
H,3.3155902344,0.2342912284,1.998707005
H,2.4512209498,0.3570700036,3.4163637774
C,-0.583104335,-0.0117751739,3.5183702189
O,-1.7041784151,0.4328662,3.7802706242
N,0.2567816991,-0.5007506622,4.4886513805
H,-0.1694576722,-0.6271196872,5.405181718
H,0.9166650995,-1.2260175078,4.2232219643

A2d

0,1
C,0.0074278458,-0.0050328388,0.0131596547
C,-0.0042160187,0.023488016,2.1645625928
C,1.3376446869,0.0111767093,1.7821028605
N,1.3144819112,-0.0046436585,0.4149736616
H,2.1386298178,0.0234787315,-0.1997189859
H,-0.2754320774,-0.0489858973,-1.0329291653
N,-0.8194359541,0.0274200803,1.0451338185
N,2.5337462454,0.1637694407,2.4756253359
H,3.2627561621,-0.4828875161,2.1714226423
H,2.4143945885,0.1078001316,3.4814561874
C,-0.5669645765,0.0829351445,3.5230917304
O,-1.6244996711,0.6625488314,3.7797084543
N,0.2062486248,-0.5033554092,4.4940261554
H,-0.2177732632,-0.5501575521,5.4193233655
H,0.7482257388,-1.3231413851,4.2309616903

RTS1**(A1,A1d')**
0,1
C,0.0099454029,0.0070117648,0.0100966322
C,-0.0107844333,0.0033504828,2.1606294213
C,1.3401385367,-0.0023470184,1.7755018489
N,1.3243980749,-0.0095158924,0.4149700579
H,2.1479524211,-0.0211952948,-0.2015629319
H,-0.2627151864,0.0155965228,-1.0398734173
N,-0.8225592021,0.0161164315,1.0318171782
N,2.4901001077,-0.0983856317,2.5161362806

H,3.3153769308,0.3253115429,2.0934769546
H,2.3546327695,0.1642558536,3.4877692467
C,-0.4570719482,0.0455780421,3.5327922679
O,0.3520735637,0.0369612526,4.4660887788
N,-1.87929469,0.0969526884,3.7421848826
H,-2.1136389256,-0.6968866252,4.3480100317
H,-2.0574791037,0.924156038,4.3219441366

RTS2**(A1,A1d')**
0,1
C,0.0105251715,0.0119013836,0.0127891618
C,-0.013937937,0.0000700428,2.1635571769
C,1.3350961088,-0.0041097829,1.7849852867
N,1.3219215811,-0.00601587,0.4229585793
H,2.1474274202,-0.0163127539,-0.1914384215
H,-0.2598694099,0.0249052649,-1.0376270877
N,-0.8238038585,0.0167242921,1.0348119876
N,2.4840418554,-0.1052401948,2.5298069405
H,3.3055620481,0.3340437618,2.1154020451
H,2.345030285,0.1547130752,3.5019662933
C,-0.5003218288,0.0356864588,3.5274631053
O,0.276505137,0.0194424196,4.4812871508
N,-1.9195229875,0.0910075981,3.7494440077
H,-2.2817101855,0.9081176548,3.2470296008
H,-2.3409036956,-0.7072134693,3.2629359643

RTS(**A2, A2d')**
0,1
C,0.004652274,0.004576033,0.0086083904
C,-0.0066661142,-0.0269286876,2.1605262886
C,1.3439158209,-0.0096282049,1.7719663854
N,1.3185186285,0.0027447461,0.4093236503
H,2.1408202445,-0.0004470044,-0.2089820443
H,-0.2728258219,0.0283052287,-1.0400665253
N,-0.8220552392,-0.0167245832,1.0332230989
N,2.5149715758,-0.1128198025,2.4840543384
H,3.3003405851,0.4019543677,2.0869005372
H,2.3515744539,0.0807926597,3.4689321838
C,-0.540436906,-0.0061196416,3.5037625425
O,-1.7377805167,-0.041157909,3.7653953787
N,0.4800822111,0.0683153633,4.5326314208
H,0.2747289853,0.9098581007,5.0836325804
H,0.3069594771,-0.7112336957,5.1773571245

CC-RTS**(A1,A2')**

0,1
C,1.836492244,-1.2875472745,0.0374070739
C,-0.0727464507,-0.2990986467,-0.0348636306

C,0.8786246103,0.7086415885,-0.0129740214
N,2.0829059565,0.0523956087,0.0259101353
H,3.0079984048,0.5006297952,0.02570328
H,2.6282020097,-2.0264988235,0.0885044642
N,0.5316954699,-1.540649629,-0.0107884724
N,0.8133670229,2.1036432736,-0.1097011117
H,-0.1381499482,2.4267623243,-0.2797891221
H,1.1713440846,2.5655438424,0.7282618628
C,-1.5533603898,-0.1547835833,-0.1243128365
O,-2.1454495881,-0.1114530332,-1.2086199891
N,-2.1813275368,-0.054730723,1.0668043201
H,-1.6678850636,-0.1957621851,1.9312133193
H,-3.199124632,-0.0385657032,1.0960744346

AICA Minima and Transition States in Acetonitrile

A1

0,1
C,0.0161164702,0.0170949738,0.0095551085
C,-0.0146912246,-0.0077110724,2.160182568
C,1.329188975,-0.0115013279,1.7918381907
N,1.3211675209,-0.0080209228,0.4256960816
H,2.150286722,-0.0166753915,-0.1842620755
H,-0.253059459,0.0380250371,-1.0410203698
N,-0.8212647774,0.0167969714,1.0333383096
N,2.4888476292,-0.1248958138,2.5351700432
H,3.2740844996,0.4058500734,2.1567066311
H,2.3239611688,0.0957518765,3.5136633471
C,-0.5217729035,0.0216586638,3.5292807684
O,0.2479954161,-0.0431767828,4.5041086727
N,-1.8650172776,0.1715185876,3.6615092563
H,-2.458484112,0.0288109183,2.8511877117
H,-2.2666644055,0.0057796514,4.580850745

A1d

0,1
C,0.0156127313,-0.0012437369,0.0090455381
C,-0.0145007631,0.020873086,2.1599163689
C,1.3293034925,0.0074142679,1.7910244205
N,1.3210503842,0.0088964074,0.4250171847
H,2.1500885169,0.0105872533,-0.1853658997
H,-0.2539746809,-0.0166078676,-1.0415097113
N,-0.8214733241,0.0055609511,1.0329997635
N,2.4891875185,0.1043153852,2.5356888916
H,3.2755020635,-0.4149582028,2.1438512425
H,2.32592572,-0.1393722444,3.5089470541
C,-0.5216376482,-0.0266659107,3.5282698868
O,0.2514960023,-0.0448170649,4.5025694992
N,-1.8730215181,0.0007041267,3.6629583839

H,-2.4510948986,-0.1882499861,2.8509172841
H,-2.2559630209,-0.219912658,4.578897424

A2

0,1
C,0.0071735086,0.0577906944,0.0131569549
C,-0.0195498944,0.0036205514,2.1648160138
C,1.3248878765,-0.0142326216,1.7886118425
N,1.3123401757,0.0103726178,0.4233111089
H,2.1410806804,0.0268788787,-0.1881441286
H,-0.2666266705,0.0812479423,-1.0361426355
N,-0.8255917392,0.0639485399,1.0397677825
N,2.5034890737,-0.1171792599,2.5175303014
H,3.3186707092,0.2034748117,1.9921506135
H,2.4593236966,0.3750133393,3.4085927926
C,-0.5868942359,-0.0166619196,3.518288589
O,-1.7144018546,0.4165249915,3.7762524008
N,0.2520208389,-0.4984794138,4.4905974064
H,-0.1741788139,-0.6313118312,5.4064519672
H,0.9313527414,-1.2066392797,4.2278284652

A2d

0,1
C,0.0083607698,-0.0030629239,0.0139653291
C,-0.0058789519,0.0220743601,2.1659822131
C,1.3366673881,0.008978358,1.7844499913
N,1.3147368653,-0.0041516245,0.4175828692
H,2.1403649697,0.0186247294,-0.1968524362
H,-0.2728992763,-0.0441766226,-1.0327930427
N,-0.8197799314,0.0277555621,1.0450698855
N,2.5315286799,0.1603023448,2.4784684311
H,3.2733344026,-0.4577199295,2.1461496647
H,2.4224119709,0.0683992145,3.4827802757
C,-0.5713406509,0.0811139078,3.5226938324
O,-1.6348832269,0.6540867911,3.7743924789
N,0.2020990289,-0.4952550927,4.4977150439
H,-0.2229054986,-0.5413945255,5.4228430467
H,0.7534175211,-1.3111617209,4.2404524158

RTS1**(A1,A1d')**

0,1
C,0.0103011077,0.0071377459,0.0110525239
C,-0.0110360119,0.0038522083,2.1620301913
C,1.3401387579,-0.0021447143,1.7766009206
N,1.3242161772,-0.0097531431,0.4162961867
H,2.1488499035,-0.0185209498,-0.2006283043
H,-0.2619237118,0.0154263997,-1.0392324109

N,-0.8226384914,0.0166293267,1.0327480934
N,2.4903989625,-0.0980000177,2.5161489292
H,3.3176629512,0.3161218458,2.0868725022
H,2.3602885136,0.1736793064,3.4862156608
C,-0.4584319238,0.0450217621,3.5334820477
O,0.3495324353,0.034931355,4.4680031441
N,-1.8808600883,0.0968451932,3.7414846426
H,-2.1163045488,-0.6977995791,4.3463774142
H,-2.0591197149,0.9235334182,4.3225298273

RTS2**(A1,A1d')**

0,1
C,0.011015745,0.0127996215,0.0136023242
C,-0.0146965339,0.0014780448,2.1646357915
C,1.3347501849,-0.0039974568,1.7861625896
N,1.3219132621,-0.0064461197,0.4244264387
H,2.1487149313,-0.0142502669,-0.1900443898
H,-0.2586099084,0.0255604969,-1.037220309
N,-0.8240692713,0.0187041832,1.0352195286
N,2.4835298084,-0.1055453744,2.5305957985
H,3.3079793158,0.3220743941,2.1087896363
H,2.3496557678,0.1662816767,3.5004235657
C,-0.5017688427,0.0354561949,3.527717717
O,0.2742465661,0.0188012314,4.4826899819
N,-1.921089927,0.089280957,3.7493578455
H,-2.2837828543,0.9066979582,3.2470931741
H,-2.3417485394,-0.7091756603,3.2619220983

RTS(**A2, A2d')**
0,1
C,0.0048896136,0.004314285,0.0092399355
C,-0.0070210037,-0.0282933082,2.1615738507
C,1.3438416474,-0.0098822051,1.7727263116
N,1.318293677,0.0027195214,0.410326436
H,2.1416211063,0.0041881216,-0.2084166256
H,-0.272144076,0.0281385207,-1.0397548989
N,-0.8222228154,-0.0179446468,1.0338017622
N,2.5146708901,-0.1119456149,2.4840281933
H,3.3027146059,0.3948388004,2.08100082
H,2.3554049954,0.0865457316,3.4685090578
C,-0.540914709,-0.006427336,3.5041241311
O,-1.7392394993,-0.0403550732,3.7646356964
N,0.4782235259,0.0678005205,4.5331691141
H,0.2733510446,0.9097920848,5.0842129233
H,0.3053306554,-0.7120024318,5.1780886428

CC-RTS**(A1,A2')**
0,1
C,1.8549352151,-1.2698283869,-0.0053349258
C,-0.0745095527,-0.3182020532,-0.053890651
C,0.8563217256,0.7069134828,0.0081231675
N,2.0733663843,0.0749878621,0.0307699653
H,2.9901934901,0.5412230837,0.0586671657
H,2.662178303,-1.9931683105,0.0248971598
N,0.5560227293,-1.5476550672,-0.068943283
N,0.7600951819,2.1012473215,-0.0468849184
H,-0.2077328122,2.4117640574,-0.1276053944
H,1.1800248783,2.5486668456,0.7703608277
C,-1.5569153343,-0.2025783884,-0.1510107528
O,-2.1394698752,-0.1224278224,-1.2394270137
N,-2.198741513,-0.1777068446,1.0352290011
H,-1.6884129113,-0.3258970887,1.9007287355
H,-3.217209419,-0.1732370692,1.0566325785

AICA Minima and Transition States in Chloroform

A1

0,1
C,-0.0052116957,-0.0075736374,-0.0047232603
C,0.0049176407,-0.0059210713,2.1440307686
C,1.3403649944,0.0010376175,1.7548897366
N,1.3092515371,-0.0101456632,0.3874733556
H,2.1220865347,-0.0428750703,-0.2318508703
H,-0.294944889,-0.0021562084,-1.0485597157
N,-0.8226222094,-0.0058358389,1.033776038
N,2.5123752433,-0.0906913613,2.4854743328
H,3.2529268038,0.524676752,2.1549683435
H,2.3248937747,0.0530766762,3.4741958018
C,-0.4731361794,0.0384274044,3.5253186213
O,0.3132379709,-0.0228786431,4.483230272
N,-1.814347086,0.2002458772,3.6761773727
H,-2.4145388807,0.054269506,2.8734600411
H,-2.2016398406,0.0421449773,4.6000294155

A1d

0,1
C,0.0106711498,-0.002471934,0.0042419058
C,-0.0088946698,0.0103716322,2.152997866
C,1.3317815715,0.0064385402,1.7823080109
N,1.3196254965,0.0094050863,0.4145527802
H,2.1405420275,0.0464899925,-0.1936409226
H,-0.2648087728,-0.01768863,-1.0433176867

N,-0.8210124759,-0.002232564,1.0312987962
N,2.4925620752,0.1087372631,2.5294603152
H,3.2463769532,-0.4925171757,2.2029623116
H,2.2930419582,-0.0517972836,3.5133053771
C,-0.5068008678,-0.0408881196,3.5270858209
O,0.269811978,-0.0743337999,4.4946149851
N,-1.8581863193,-0.0053816929,3.6631492737
H,-2.4357140787,-0.1680617429,2.8473627031
H,-2.2424954501,-0.2195457655,4.5768457942

A2

0,1
C,0.0044414963,0.0380343062,0.0079358768
C,-0.0142566409,-0.0072059613,2.1568168064
C,1.3286941707,-0.0132491725,1.7805406336
N,1.3144420821,0.0038295543,0.4137410921
H,2.1346658393,0.0082148922,-0.1970680933
H,-0.2732260884,0.0558359601,-1.0391043322
N,-0.8238929603,0.0401491839,1.0350311757
N,2.514343615,-0.0993627458,2.5048726111
H,3.2946427959,0.3606471693,2.0386113373
H,2.4133946492,0.2735121844,3.4451274038
C,-0.5672187699,0.0084584214,3.5180874949
O,-1.6614337504,0.4932784127,3.7966218141
N,0.2806236331,-0.5071957456,4.480064588
H,-0.1443841907,-0.6085421785,5.3985987902
H,0.8622602114,-1.2920362397,4.2031922759

A2d

0,1
C,0.0031057254,-0.0043659921,0.0075892053
C,0.0015260336,0.0194132679,2.156024976
C,1.3410314482,0.0125609445,1.7706421809
N,1.312882749,-0.0005373269,0.4018813179
H,2.1309369672,0.0592035013,-0.2089695448
H,-0.2870453013,-0.0465800909,-1.0354622213
N,-0.8186013849,0.0235297577,1.0430322365
N,2.5475031244,0.1532026528,2.4599559158
H,3.1916841445,-0.6206986359,2.3033311517
H,2.3965719435,0.2760346926,3.4559751409
C,-0.5544771153,0.0797766873,3.5213222699
O,-1.6016822989,0.6618688129,3.7898322977
N,0.2307811872,-0.5156054312,4.4855245252
H,-0.1988744651,-0.5777786928,5.4052119403
H,0.7598913027,-1.3356113191,4.2070086064

RTS1**(A1,A1d')**
0,1
C,0.0069141344,0.0053270444,0.0067367475
C,-0.0076824135,0.0000272157,2.1547617449
C,1.3413057713,-0.0027535026,1.7702113468
N,1.3246856736,-0.0071959749,0.4083439113
H,2.1420191099,-0.0370414669,-0.2055863245
H,-0.2690473016,0.0154571286,-1.0411270732
N,-0.8220675859,0.0115331064,1.0293986166
N,2.4920876283,-0.0992827721,2.5141331898
H,3.300664584,0.3818201407,2.1282399869
H,2.3293695282,0.1134110202,3.4935296515
C,-0.448797756,0.045508468,3.5309044168
O,0.3641156213,0.0364731255,4.459371438
N,-1.8701704648,0.1017216541,3.7434555517
H,-2.1061678636,-0.6886473549,4.3497679063
H,-2.0461543477,0.9306023251,4.3178402582

RTS2**(A1,A1d')**
0,1
C,0.0076992717,0.0092389877,0.0082783708
C,-0.0100568973,-0.0026144023,2.1575668569
C,1.3364877781,-0.0043648966,1.7787285
N,1.321650099,-0.0048778511,0.4150728206
H,2.1406027498,-0.0339973173,-0.1972708796
H,-0.2666496253,0.0234155279,-1.0398535689
N,-0.8228361181,0.0118743879,1.0323094626
N,2.4865415584,-0.1061342262,2.5260579256
H,3.2886801529,0.3959722791,2.1530921567
H,2.3190434862,0.0961101095,3.5070791901
C,-0.4919293041,0.0385914188,3.5269474501
O,0.2896219538,0.0252585401,4.4740979357
N,-1.9105181968,0.0973375904,3.7511239711
H,-2.270462555,0.9115357691,3.2460210231
H,-2.3318346488,-0.6996260364,3.2661205763

RTS(**A2, A2d')**
0,1
C,0.003283636,0.0053186271,0.0057505132
C,-0.0042179012,-0.0189014624,2.1554574894
C,1.3447795252,-0.0081588776,1.7686149798
N,1.319591413,0.001746754,0.4045254657
H,2.1365986235,-0.0282003432,-0.2098698697
H,-0.2767463187,0.0281765098,-1.0410187585
N,-0.8208188363,-0.0097321867,1.0307298483
N,2.5192230954,-0.1150323774,2.4820253838
H,3.2857523133,0.4442360134,2.1147640088
H,2.3384538942,0.0513661368,3.4695073235
C,-0.5389048245,-0.0034717238,3.501788085

O,-1.7313072633,-0.0408365593,3.7679155297
N,0.4884097484,0.0677923869,4.5311575969
H,0.2826213058,0.9070725709,5.0820191108
H,0.3100812473,-0.7098884983,5.1738986436

CC-RTS**(A1,A2')**

0,1
C,1.8665295396,-1.2475322066,0.1015012557
C,-0.0613195833,-0.3108828725,-0.0166079463
C,0.8640109781,0.7216878246,-0.0454838599
N,2.0835936579,0.0910103024,0.0286513916
H,2.9877402468,0.5688081115,0.0126232896
H,2.6699026264,-1.9705065273,0.1741403161
N,0.5647436106,-1.532046511,0.0738125676
N,0.7824087992,2.1245212481,-0.1563398165
H,0.2424647476,2.396868693,-0.9761603024
H,0.3530289146,2.5435629459,0.6664471313
C,-1.5444906986,-0.1905376088,-0.1188059576
O,-2.1369236667,-0.2754197936,-1.1944149227
N,-2.1689243874,0.0643413309,1.0594389938
H,-1.6668297311,-0.0709960121,1.9290606809
H,-3.1843594548,0.0295160685,1.0834324796